

AD-A023 355

AN EXPERIMENTAL INVESTIGATION OF PRESSURE OSCILLATIONS
IN TWO-DIMENSIONAL OPEN CAVITIES

Michael F. Marquardt

Air Force Institute of Technology
Wright-Patterson Air Force Base, Ohio

December 1975

DISTRIBUTED BY:

NTIS

National Technical Information Service
U. S. DEPARTMENT OF COMMERCE

KEEP UP TO DATE

Between the time you ordered this report—which is only one of the hundreds of thousands in the NTIS information collection available to you—and the time you are reading this message, several *new* reports relevant to your interests probably have entered the collection.

Subscribe to the **Weekly Government Abstracts** series that will bring you summaries of new reports as soon as they are received by NTIS from the originators of the research. The WGA's are an NTIS weekly newsletter service covering the most recent research findings in 25 areas of industrial, technological, and sociological interest—invaluable information for executives and professionals who must keep up to date.

The executive and professional information service provided by NTIS in the **Weekly Government Abstracts** newsletters will give you thorough and comprehensive coverage of government-conducted or sponsored re-

search activities. And you'll get this important information within two weeks of the time it's released by originating agencies.

WGA newsletters are computer produced and electronically photocomposed to slash the time gap between the release of a report and its availability. You can learn about technical innovations immediately—and use them in the most meaningful and productive ways possible for your organization. Please request NTIS-PR-205/PCW for more information.

The weekly newsletter series will keep you current. But *learn what you have missed in the past* by ordering a computer **NTISearch** of all the research reports in your area of interest, dating as far back as 1964, if you wish. Please request NTIS-PR-186/PCN for more information.

WRITE: Managing Editor
5285 Port Royal Road
Springfield, VA 22161

Keep Up To Date With SRIM

SRIM (Selected Research in Microfiche) provides you with regular, automatic distribution of the complete texts of NTIS research reports *only* in the subject areas you select. SRIM covers almost all Government research reports by subject area and/or the originating Federal or local government agency. You may subscribe by any category or subcategory of our WGA (**Weekly Government Abstracts**) or **Government Reports Announcements and Index** categories, or to the reports issued by a particular agency such as the Department of Defense, Federal Energy Administration, or Environmental Protection Agency. Other options that will give you greater selectivity are available on request.

The cost of SRIM service is only 45¢ domestic (60¢ foreign) for each complete

microfiched report. Your SRIM service begins as soon as your order is received and processed and you will receive biweekly shipments thereafter. If you wish, your service will be backdated to furnish you microfiche of reports issued earlier.

Because of contractual arrangements with several Special Technology Groups, not all NTIS reports are distributed in the SRIM program. You will receive a notice in your microfiche shipments identifying the exceptionally priced reports not available through SRIM.

A deposit account with NTIS is required before this service can be initiated. If you have specific questions concerning this service, please call (703) 451-1558, or write NTIS, attention SRIM Product Manager.

This information product distributed by

NTIS

U.S. DEPARTMENT OF COMMERCE
National Technical Information Service
5285 Port Royal Road
Springfield, Virginia 22161

Unclassified

SECURITY CLASSIFICATION OF THIS PAGE (When Data Entered)

REPORT DOCUMENTATION PAGE		READ INSTRUCTIONS BEFORE COMPLETING FORM
1. REPORT NUMBER GAE/AE/75D-14	2. GOVT ACCESSION NO.	3. REGISTRY CATALOG NUMBER AD A023355
4. TITLE (and Subtitle) AN EXPERIMENTAL INVESTIGATION OF PRESSURE OSCILLATIONS IN TWO-DIMENSIONAL OPEN CAVITIES		5. TYPE OF REPORT & PERIOD COVERED AFIT Thesis
		6. PERFORMING ORG. REPORT NUMBER
7. AUTHOR(s) Michael F. Marquardt Captain USAF		8. CONTRACT OR GRANT NUMBER(s)
9. PERFORMING ORGANIZATION NAME AND ADDRESS Air Force Institute of Technology (AU) Wright-Patterson AFB, Ohio 45433		10. PROGRAM ELEMENT, PROJECT, TASK AREA & WORK UNIT NUMBERS
11. CONTROLLING OFFICE NAME AND ADDRESS		12. REPORT DATE December 1975
		13. NUMBER OF PAGES 68
14. MONITORING AGENCY NAME & ADDRESS (if different from Controlling Office)		15. SECURITY CLASS. (of this report) Unclassified
		15a. DECLASSIFICATION DOWNGRADING SCHEDULE
16. DISTRIBUTION STATEMENT (of this Report) Approved for public release; distribution unlimited.		
17. DISTRIBUTION STATEMENT (of the abstract entered in Block 20, if different from Report) NOT SUBJECT TO CONTROL		
18. SUPPLEMENTARY NOTES Approved for public release; TAW AFR/190-17 Jerry C. Hix, Captain, USAF Director of Information		
19. KEY WORDS (Continue on reverse side if necessary and identify by block number) Cavity Oscillations Cavity Flow Shear Layer REPRODUCED BY NATIONAL TECHNICAL INFORMATION SERVICE U. S. DEPARTMENT OF COMMERCE SPRINGFIELD, VA. 22161		
20. ABSTRACT (Continue on reverse side if necessary and identify by block number) An experimental study was conducted to determine the characteristics of the pressure oscillations in a small two-dimensional cavity exposed to tangential air flow. Various cavity configuration changes, involving the shape of the leading and trailing edge, were investigated to determine the relative capability to suppress the resonance in the cavity response.		

DD FORM 1 JAN 73 1473

EDITION OF 1 NOV 65 IS OBSOLETE

Unclassified

SECURITY CLASSIFICATION OF THIS PAGE (When Data Entered)

Unclassified

SECURITY CLASSIFICATION OF THIS PAGE(When Data Entered)

Five airflow Mach numbers (0.5, 0.6, 1.0, 1.3, 1.5) were used to investigate the Mach-response relationship. Two cavity lengths were considered (2 and 4 1/4 inches). The depth of the cavities was kept constant at one inch.

Fluctuating pressure recordings and schlieren photographs were made of each test. A narrow-band analysis of the recordings produced plots of amplitude vs frequency. These were used to compare the cavity responses.

A 15° ramp inclined into the cavity at the leading edge produced the most significant suppression in the short cavity (L/D = 2). In the long cavity (L/D = 4 1/4) this ramp augmented the cavity response. Increasing the angle of a trailing edge ramp (up to 45°) was found to have increasing suppression effects, particularly for the short cavity.

h a

Unclassified

SECURITY CLASSIFICATION OF THIS PAGE(When Data Entered)

ACCESSION NO.	
DTIC	Watts Section <input checked="" type="checkbox"/>
	Ball Section <input type="checkbox"/>
A	

AN EXPERIMENTAL INVESTIGATION
 OF PRESSURE OSCILLATIONS IN
 TWO-DIMENSIONAL OPEN CAVITIES

THESIS

GAE/AE/75D-14

Michael F. Marquardt
 Captain USAF

DTIC
 REPRODUCED
 A

Approved for public release; distribution unlimited.

u-b

AN EXPERIMENTAL INVESTIGATION OF
PRESSURE OSCILLATIONS IN TWO-
DIMENSIONAL OPEN CAVITIES

THESIS

Presented to the Faculty of the School of Engineering
of the Air Force Institute of Technology
Air University
in Partial Fulfillment of the
Requirements for the Degree of
Master of Science

by

Michael F. Marquardt, B.Aero.E.

Captain USAF

Graduate Aeronautical Engineering

December 1975

Approved for public release; distribution unlimited.

M.C.

Preface

Rectangular cavities exposed to air flowing across the opening respond by generating pressure fluctuations at levels and frequencies that are perceived as noise. Certain conditions of flow velocity and cavity geometry can create resonant responses at discrete frequencies (tones) inside the cavity. These tones can produce sound pressure level amplitudes which can adversely affect the integrity of the structure containing the cavity. In this study, I investigated the response characteristics of several rectangular cavities at various flow velocities and the effectiveness of certain cavity modifications intended to suppress the level of the cavity response.

I would like to express my appreciation to my advisor, Dr. M. E. Franke, who guided me in selecting and limiting the variables considered in this study and for the discussions which clarified the fundamental concepts involved in this study. I would like to thank Capt. D. L. Carr of AFFDL for his assistance concerning the operation of the equipment used on this project and for his advice concerning the utilization of the final machine plots. I also want to thank Mr. S. M. Bower of AFFDL for his work in converting magnetic tape data into the plots needed for this study and for his assistance in identifying anomalies in the data and discussing potential sources of anomalies in the results.

I want to thank Mr. J. T. Flahive and Mr. W. W. Baker for their assistance with the laboratory equipment. I also want to thank Mr. M. W. Wolfe for his guidance and for the work performed in the AFIT shop.

Michael F. Marquardt

Contents

Preface	11
List of Figures	iv
List of Tables	vi
List of Symbols	vii
Abstract	viii
I. Introduction	1
Background	1
Objective	2
Scope	2
II. Discussion of Cavity Flow	5
Physical Mechanisms	5
Oscillation Suppression	6
III. Experimental Equipment	9
Test Section Assembly	9
Air Supply System	12
IV. Experimental Procedures	19
V. Results and Discussion	22
Test Conditions	22
Resonant Frequencies	22
Mach Number Effect on Fluctuating Pressure Levels	24
Suppression Effectiveness on Fluctuating Pressure Levels	25
L/D = 2 Cavities	25
L/D = 4 1/4 Cavities	32
Modes of Fluctuating Pressure Levels	33
Narrow-band Spectra of Fluctuating Pressure Levels	34
L/D = 2 Cavities	34
Tandem L/D = 2 Cavities	46
L/D = 4 1/4 Cavities	46
VI. Conclusions	53
Bibliography	54
Vita	55

List of Figures

<u>Figure</u>		<u>Page</u>
1	Cavity Geometry Nomenclature	4
2	Two-Dimensional Open Cavity	8
3	Two-Dimensional Closed Cavity	8
4	Photograph of Test Section Assembly with Nozzle and Cavity Components	10
5	L/D = 2 Cavity Configurations	13
6	Double Cavity (Tandem) Configurations	14
7	L/D = 4.25 Cavity Configurations with Straight Leading Edge	15
8	L/D = 4.25 Cavity Configurations with 15 Degree, 1 Inch, Leading Edge Ramp	16
9	Microphone Identities and Locations in Each Basic Cavity Configuration.	17
10	Schematic of the Schlieren Apparatus.	21
11	Nondimensional Resonant Frequencies as a Function of Mach Number with Implementation of Rossiter's Formula	28
12	Nondimensional Resonant Frequencies as a Function of Mach Number with Implementation of Modified Rossiter Formula.	29
13	Maximum Dynamic Pressure Amplitude Variation with Mach Number for L/D = 2 Cavities	30
14	Maximum Dynamic Pressure Amplitude Variation with Mach Number for L/D = 4.25 Cavities	31
15	Range of Maximum Sound Pressure Levels in the Rectangular L/D = 2 Cavity as a Function of Mach Number	35
16	Range of Maximum Sound Pressure Levels in the L/D = 2 Cavity with 25°, 1 inch, Trailing Edge Ramp as a Function of Mach Number	36
17	Range of Maximum Sound Pressure Levels in the L/D = 2 Cavity with 45°, 1/2 inch, Trailing Edge Ramp as a Function of Mach Number	37

<u>Figure</u>		<u>Page</u>
18	Range of Maximum Sound Pressure Levels in the L/D = 4.25 Rectangular Cavity as a Function of Mach Number.	38
19	Range of Mode-1 Sound Pressure Levels in the L/D = 4.25 Cavity with 45°, 1 inch, Trailing Edge Ramp	39
20	Sound Pressure Level (SPL) Variation with Frequency in the L/D = 2 Rectangular Cavity at M = 1.5, 1.3, and 1.0	40
21	Sound Pressure Level Variation with Frequency in the L/D = 2 Rectangular Cavity at M = 0.6, and 0.5	41
22	Comparison of L/D = 2 Rectangular (A) and 25° Rear Ramp (C) Cavity SPL at M = 1.5, 1.0, and 0.5	42
23	Comparison of L/D = 2 Rectangular (A) and 45°, 1/2 Inch, Rear Ramp (F) Cavity SPL at M = 1.5, 1.0, and 0.6	43
24	Comparison of L/D = 2 Rectangular (A) and 45°, 1 Inch, Rear Ramp (E) Cavity SPL at M = 1.5 and 1.3	44
25	Comparison of SPL in L/D = 2 Cavities with and Without Leading Edge Ramp at M = 1.5	45
26	Sound Pressure Level Variation with Frequency in the L/D = 4.25 Rectangular Cavity at M = 1.5	48
27	Sound Pressure Level Variation with Frequency in the L/D = 4.25 Rectangular Cavity at M = 1.3	49
28	Sound Pressure Level Variation with Frequency in the L/D = 4.25 Rectangular Cavity at M = 1.0	50
29	Sound Pressure Level Variation with Frequency in the L/D = 4.25 Rectangular Cavity at M = 0.6	51
30	Sound Pressure Level Variation with Frequency in the L/D = 4.25 Rectangular Cavity at M = 0.5	52

List of Tables

<u>Table</u>		<u>Page</u>
I	Microphone Positions in Cavities	18
II	Mach and Reynolds Numbers Pertaining to the Test Assembly	23
III	Resonant Frequency Data for the $L/D = 2$ Rectangular Cavity	26
IV	Resonant Frequency Data for the $L/D = 4.25$ Rectangular Cavity	27

List of Symbols

<u>Symbol</u>	<u>Definition</u>
D	Cavity Depth, ft
f	Frequency, Hz
L	Cavity Length, ft
M	Mach Number, U/a
n	Integer, frequency mode number
S	Strouhal Number, $\frac{fL}{U} = \frac{n - 0.25}{M + 1.75}$
S*	Modified Strouhal Number, $\frac{fL}{U} = \frac{n - 0.25}{\frac{M}{(1 + 0.2M^2)^{1/2}} + 1.75}$
SPL	Sound Pressure Level, dB = $20 \log_{10} \frac{P_{rms}}{P_{ref}}$, $P_{ref} = 20$ micronewtons per sq. meter
U	Freestream Velocity, ft/sec
u	Mach Angle, rad

Abstract

An experimental study was conducted to determine the characteristics of the pressure oscillations in a small two-dimensional cavity exposed to tangential air flow. Various cavity configuration changes, involving the shape of the leading and trailing edge, were investigated to determine the relative capability to suppress the resonance in the cavity response.

Five airflow Mach numbers (0.5, 0.6, 1.0, 1.3, 1.5) were used to investigate the Mach-response relationship. Two cavity lengths were considered (2 and 4 1/4 inches). The depth of the cavities was kept constant at one inch.

Fluctuating pressure recordings and schlieren photographs were made of each test. A narrow band analysis of the recordings produced plots of amplitude vs frequency. These were used to compare the cavity responses.

A 15° ramp inclined into the cavity at the leading edge produced the most significant suppression in the short cavity ($L/D = 2$). In the long cavity ($L/D = 4 \frac{1}{4}$) this ramp augmented the cavity response. Increasing the angle of a trailing edge ramp (up to 45°) was found to have increasing suppression effects, particularly for the short cavity.

AN EXPERIMENTAL INVESTIGATION OF
PRESSURE OSCILLATIONS IN TWO-
DIMENSIONAL OPEN CAVITIES

I. Introduction

Background

High-speed air flow over surfaces with open cavities can produce intense discrete-frequency (tonal) pressure fluctuations. Under certain conditions, these tone pressure levels can reach such magnitude that nearby structure and instrumentation might be damaged. Pressure oscillations in aircraft weapon bays can affect the timing of weapon release and the initial trajectory of the store. Aircrew comfort and performance can also be affected.

Karamcheti (Ref 1) performed one of the first experimental studies of flow-induced oscillations in 1955. Discrete-frequency noise was detected in the cavity. Karamcheti noted that acoustic intensities were higher when the boundary layer upstream of the cavity was laminar rather than turbulent. Other investigators conducted extensive research which identified many other variables. Their work was directed toward an understanding of the mechanisms involved (Ref 2; Ref 3; Ref 4). The investigations led to a better understanding of the mechanisms and to several semi-empirical schemes that predict the resonant oscillation frequencies with satisfactory accuracy. However, the understanding of the problem has not yet advanced so that detailed design criteria are available for cavities or mechanisms which suppress

cavity pressure oscillations. Thus each new cavity design must be tested for its response.

Objective

The purpose of this investigation is to measure the pressure oscillations in a small scale two-dimensional rectangular cavity and to determine the relative effectiveness of cavity configurations designed to suppress the oscillations.

Scope

The cavities considered in this study are represented by two-dimensional cutouts, Fig. 1, with length-to-depth (L/D) ratios of 2 and $4\frac{1}{4}$. The effect of flow over two closely spaced cavities, one immediately behind the other, with $L/D = 2$ for each cavity, is also investigated. Six different cavity trailing edge shapes (ramps at different angles) and two leading edge shapes are investigated to determine the effect on oscillation suppression. Mach number effect is considered by using three different convergent-divergent nozzles designed to give Mach numbers of 1.2, 1.4, and 1.6. Higher Mach numbers with shock-free flow in the test section are not possible due to the maximum continuous pressure limit of the air supply. Subsonic flow effects, at approximately $M = 0.5$ and 0.6 , are also considered.

Schlieren photographs are used to visualize the shear layer over the cavity and any disturbances in the flow above the cavity. The flow Mach number at the cavity is determined by measuring, on the photographs, the Mach angle, μ , at the leading edge of the cavity and converting this to Mach number through the relation $\sin \mu = 1/M$.

Dynamic pressure measurements of the cavity oscillations are obtained by transducers mounted in the plexiglass sideplates of the apparatus. A narrow band (20 Hz) analysis of the recorded signals results in a plot of dynamic pressure amplitude as a function of frequency of the cavity oscillations. This analysis is performed by the Air Force Flight Dynamics Laboratory.

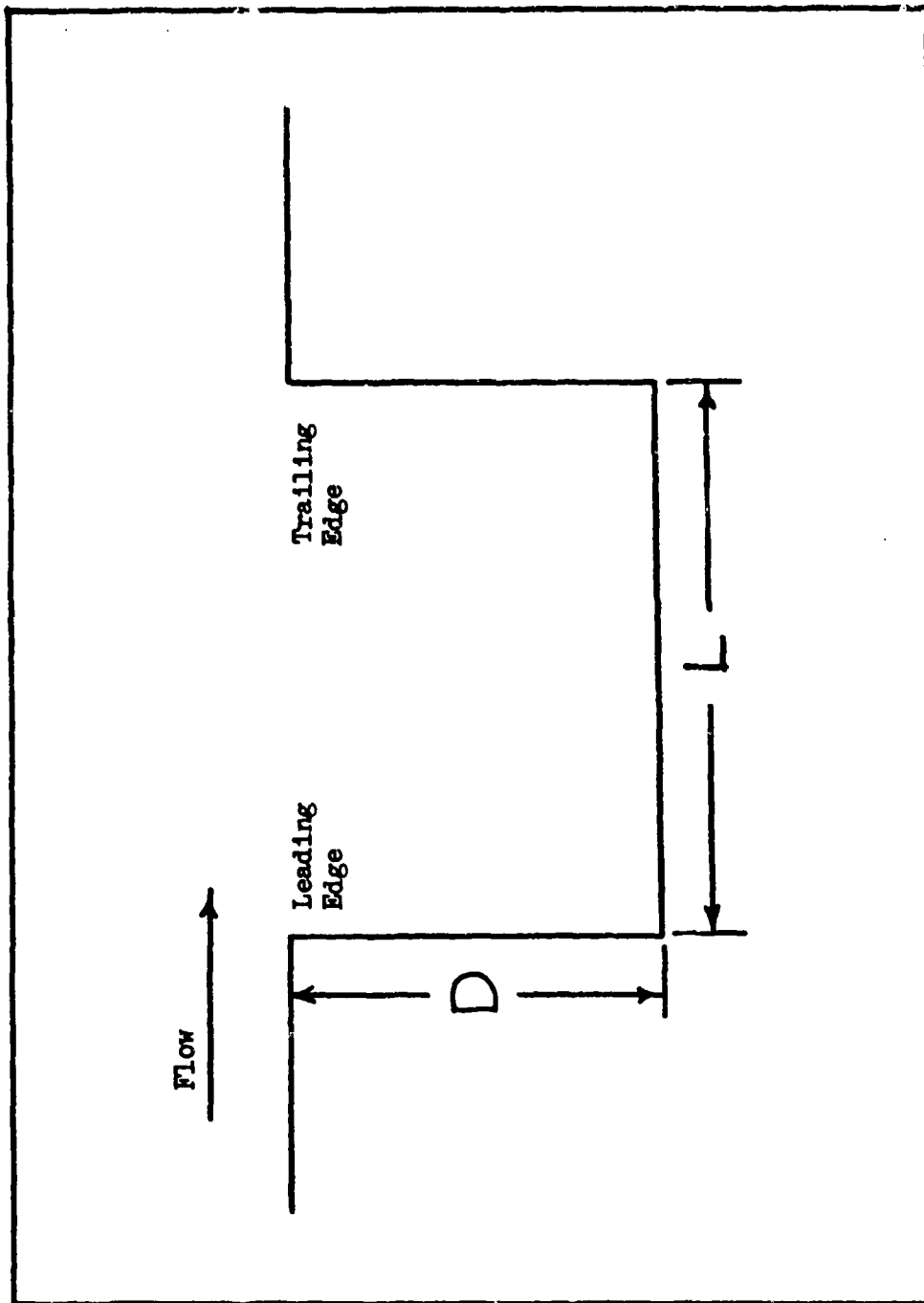


Fig. 1. Cavity Geometry Nomenclature

II. Discussion of Cavity Flow

Physical Mechanisms

Investigators using water table simulation of supersonic airflow over open cavities have identified the primary mechanisms of oscillations in cavities. Heller and Bliss (Ref 5) give a thorough discussion of the mechanisms involved. Flow over a cavity separates at the sharp leading edge. The shear layer which forms between the flow and eddying cavity fluid grows thicker in the downstream direction. The shear layer grows by entraining fluid from the flow outside and the fluid inside the cavity. If the shear layer remains steady, a fluid circulation occurs within the cavity. Fluid entrained into the shear layer is replaced by a portion of the fluid in the shear layer which turns inward at the shear layer stagnation points on the cavity trailing edge (Ref 5,7-10).

Unsteady pressure oscillations in cavities have been associated with unsteady motion of the shear layer. Study of water table simulations (Ref 5; Ref 6; Ref 7) indicated that unsteady shear layer motion causes periodic mass addition and expulsion at the cavity trailing edge. Motion picture analysis revealed the internal process. When the rear attachment point of the shear layer moves into the cavity, a small amount of fluid is added to the cavity. This fluid addition creates a pressure wave which moves through the cavity toward the leading edge from which it will be reflected. A forward moving wave trails an oblique shock into the free stream flow. This wave will cross at least one wave moving toward the trailing edge. Each reflected wave inside the cavity causes the shear layer to bulge outward so that when the wave reaches the rear face of the cavity a small amount of fluid is ejected

and the process repeats. Thus, a feedback mechanism is at work: the unsteady shear layer creates compression waves which in turn modulate the shear layer. Vortex shedding from the leading edge has been noted. This action is considered to be a manifestation of the oscillation process, but not essential to the mechanism. In subsonic flow the shear layer tends to roll up into discrete vortices. This process seems to provide an amplitude-limiting mechanism (Ref 5:19).

By convention, a cavity exposed to external flow is called open or closed depending on the behavior of the shear layer. The shear layer may either span the cavity or enter the cavity and attach to the cavity floor (Ref 8). In open cavities the shear layer spans the opening and reattaches to the trailing edge. Figure 2 depicts the open cavity. Closed cavities, shown in Fig. 3, are those in which the shear layer enters the cavity and reflects off the bottom. The closed cavity is not investigated in this study.

Oscillation Suppression

It has been found that the oscillation amplitudes can be reduced by stabilizing the shear layer or by preventing the trailing edge mass addition process or by doing both (Ref 5; Ref 7). Internal baffles and devices have had little effect (Ref 5:143-145). Spoilers installed upstream of the cavity tended to stabilize the shear layer and reduce oscillations (Ref 5:146-154). In large scale wind tunnel tests (Ref 5), trailing edge designs which reduced the fluid ingestion and stabilized the shear layer attachment point tended to give the best results. A rear-slanting ramp cut into the top of the aft end generally gave the most consistent suppression. A ramp angle of 45 degrees seemed to be

best. The rear ramp with a small thick airfoil above it seemed to control the mass injection, but its effectiveness tended to depend on location and Mach number (Ref 5:164).

Small scale tests confirmed the general effectiveness of a rear ramp (at 15 degrees) to suppress cavity oscillations (Ref 7). Additionally, it was found that a ramp (at 15 degrees) cut into the leading edge of the cavity reduced oscillation intensities when the flow separated near the leading edge of the ramp. However, under certain conditions of Mach number and geometry, the flow did not separate from the ramp and oscillations were magnified (Ref 10).

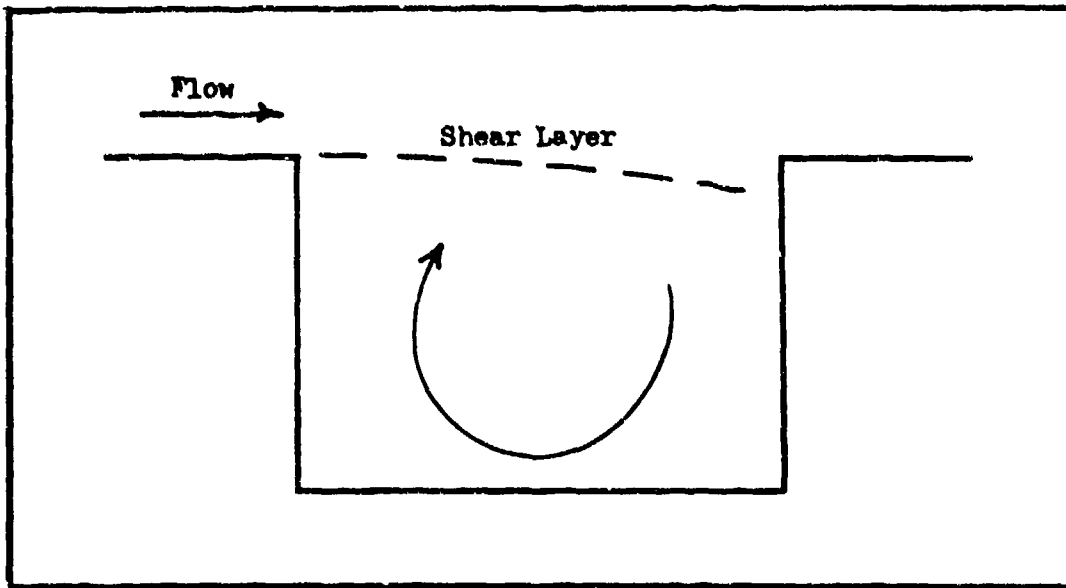


Fig. 2. Two-Dimensional Open Cavity.

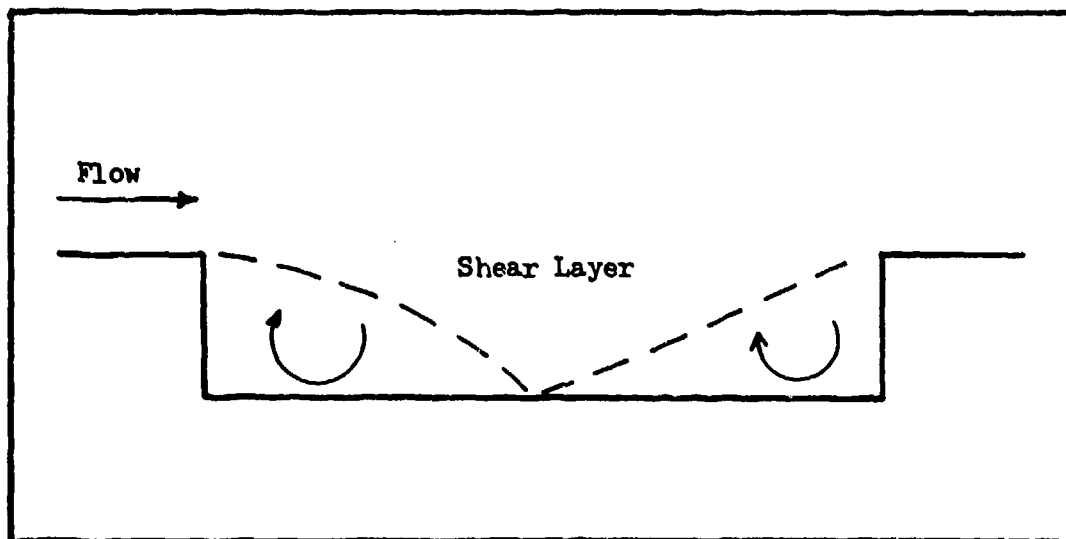


Fig. 3. Two-Dimensional Closed Cavity.

III. Experimental Equipment

The experimental equipment used in the study consisted of the test section assembly and the air supply system.

Test Section Assembly

The test section assembly, shown in Fig. 4, consisted of a two-dimensional convergent-divergent nozzle and the attached cavity model sandwiched between two pieces of 3/4 inch thick clear plexiglass. Paper gasket material was glued to the nozzle pieces and to the cavity models to provide an air-tight seal. Additionally, a rubber O-ring was installed in a groove machined into the aluminum base-plate. This reduced air leakage at the base of the assembly. The assembly was mounted on a calming chamber.

Three sets of two-dimensional nozzles, constructed from 5/16 inch aluminum, were fabricated in the Air Force Institute of Technology Shop. The shapes of the divergent portions of the nozzles (throat to exit) were determined by a computer program written by Major C. G. Stenberg of the Aero-Mechanical Department, AFIT. This program used isentropic relationships and the method of characteristics. The desired Mach numbers, 1.6, 1.4, and 1.2, were part of the input parameters used by the program. The results of the program for the iteration step size used were nozzle design Mach numbers of 1.61, 1.39, and 1.20.

The convergent section shapes of the nozzle sections were determined according to a method suggested by Professor H. G. Larsen of the Aerospace Design Center, AFIT. The surfaces of the two pieces forming each nozzle converged from parallel at the inlet to parallel at the nozzle throat in a smooth curve. The radius of curvature of the surface changed

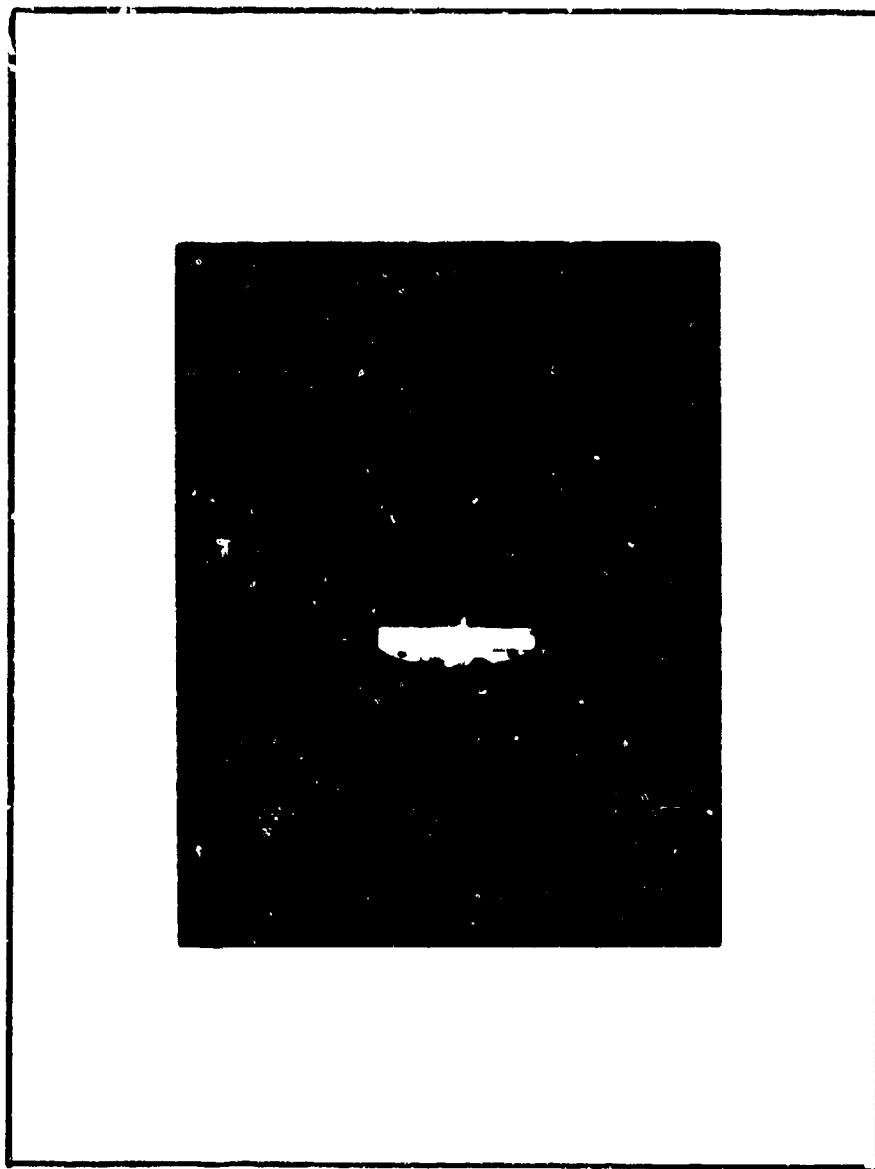


Fig. 4. Photograph of Test Section Assembly
with Nozzle and Cavity Components.

continuously from inlet to throat and the inflection point of the surface curve was located at the mid-point between the inlet and throat. This surface introduced only small disturbances to the airflow as it approached the nozzle throat.

At the suggestion of Major Stolberg, the nozzle design included a static pressure hole in each nozzle block at the nozzle exit. These pressure taps were used to set the nozzle exit static pressure equal to atmospheric pressure by controlling the total pressure in the calming chamber. Thus for each nozzle and cavity configuration the air flow at the nozzle exit reached the desired, and repeatable, Mach number and complete expansion. Achievement of complete expansion of the flow in the nozzle was necessary to eliminate any effect that flow expansion or contraction might have on the response of the cavity.

The cavity pieces were constructed of 5/16 inch thick aluminum. All cavities had a depth of one inch. The cavity trailing edge pieces, when installed, created cavity lengths of 2 and 4 1/4 inches. The cavity leading edge was located 2 inches downstream from the nozzle exit.

The cavity configurations tested were those tested by Carr (Ref 7) and other cavities which consisted of various trailing edge shapes. These shapes consisted of ramps at several different angles relative to the cavity bottom. The following is a list of the leading and trailing edge shapes for the cavities tested:

<u>Leading Edge</u>	<u>Trailing Edge</u>
straight (no ramp)	straight (no ramp)
15°, 1 in. ramp	15°, 1 in. ramp
	25°, 1 in. ramp
	35°, 1 in. ramp
	45°, 1 in. ramp
	45°, 1/2 in. ramp

A series of double cavities, each with $L/D = 2$, were created by installation of a $1/4$ inch wide divider in the $L/D = 4 \frac{1}{4}$ cavities. All of the trailing edge shapes were not included in the investigations of double cavities. Representations of the cavity configurations tested are given in Figs. 5 through 8.

The trailing edge shapes of greatest interest were the two with 45 degree ramps. This ramp angle had been found (Ref 5) to create the greatest suppression of pressure oscillations in cavities (considering only various trailing edge configurations). The $1/2$ inch ramp at 45 degrees was investigated as well as the various one inch ramps because the one inch 45 degree ramp modified the cavity to such an extent that the effective L/D , based on total volume, increased by $1/8$ in the case of the $L/D = 2$ cavity.

Holes $3/8$ inch in diameter were drilled and tapped in one piece of plexiglass so that microphones could be mounted facing the cavity side. The locations of these holes are shown in Fig. 9 and described in Table I.

Air Supply System

The compressed air system consisted of a compressor that was capable of producing 100 psi. However, the maximum continuous pressure was regulated to a lower level for each set of nozzle blocks. A filter was installed at the base of the calming chamber, to which the test assembly was attached, to remove particles and oil which might scratch the plexiglass. This filter caused a pressure drop of approximately 10 psi but did not have an adverse affect on any parameters of the experiment. The mass flow rate was sufficient to achieve sonic flow at the throat of each nozzle.

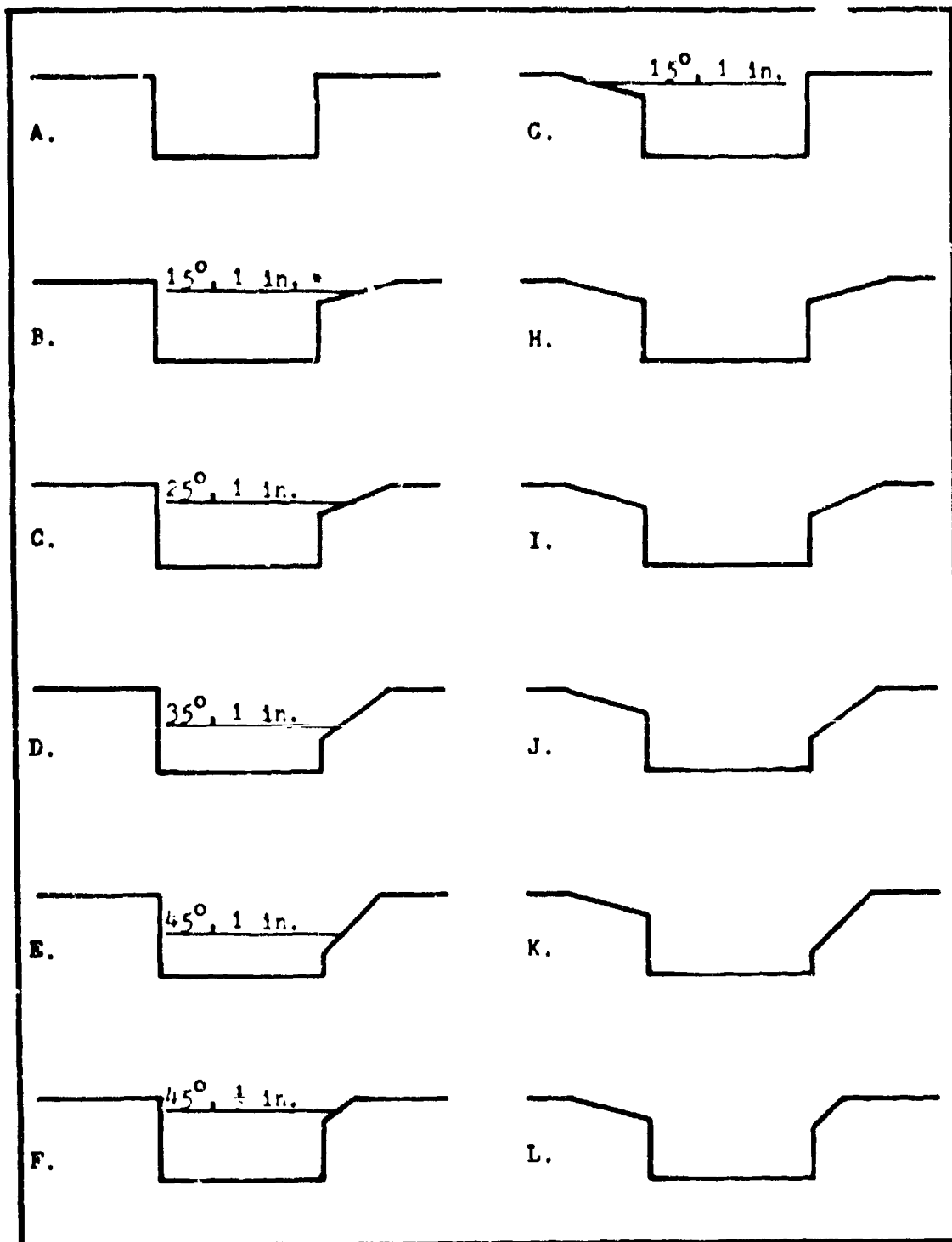


Fig. 5. $L/D = 2$ Cavity Configurations.

* Ramp lengths measured along ramp surface.

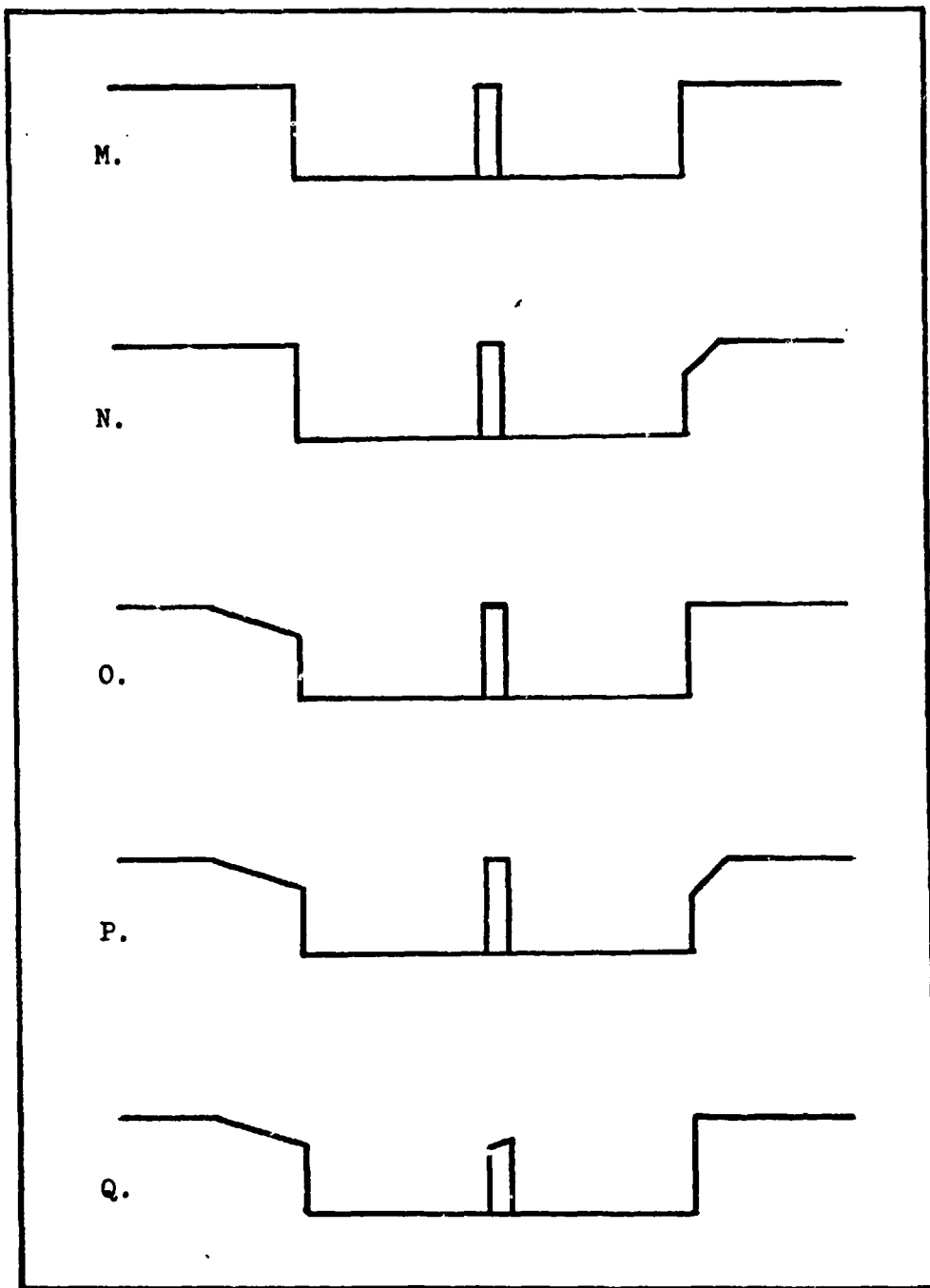


Fig. 6. Double Cavity (Tandem) Configurations.

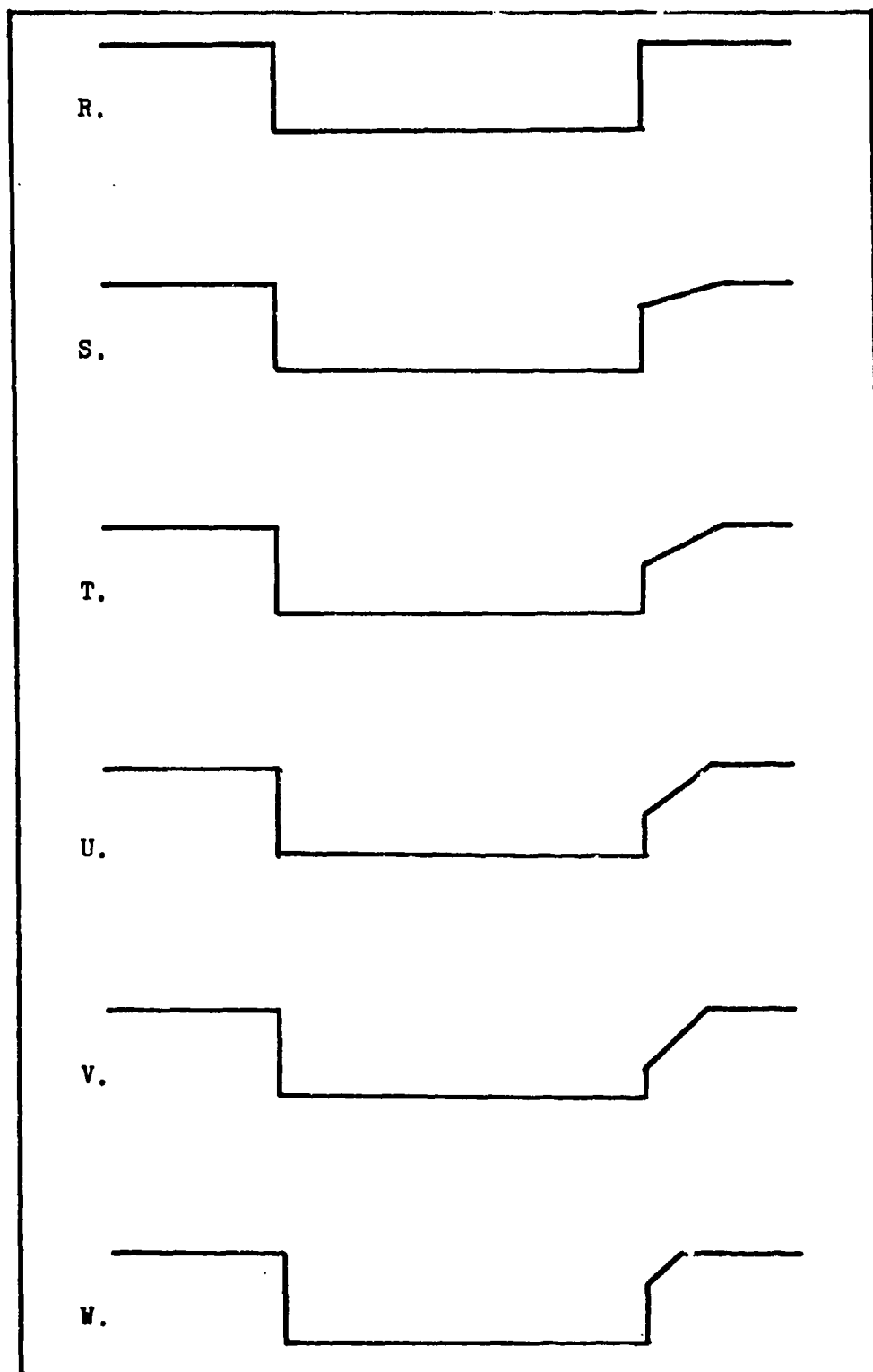


Fig. 7. $L/D = 4.25$ Cavity Configurations
with Straight Leading Edge.

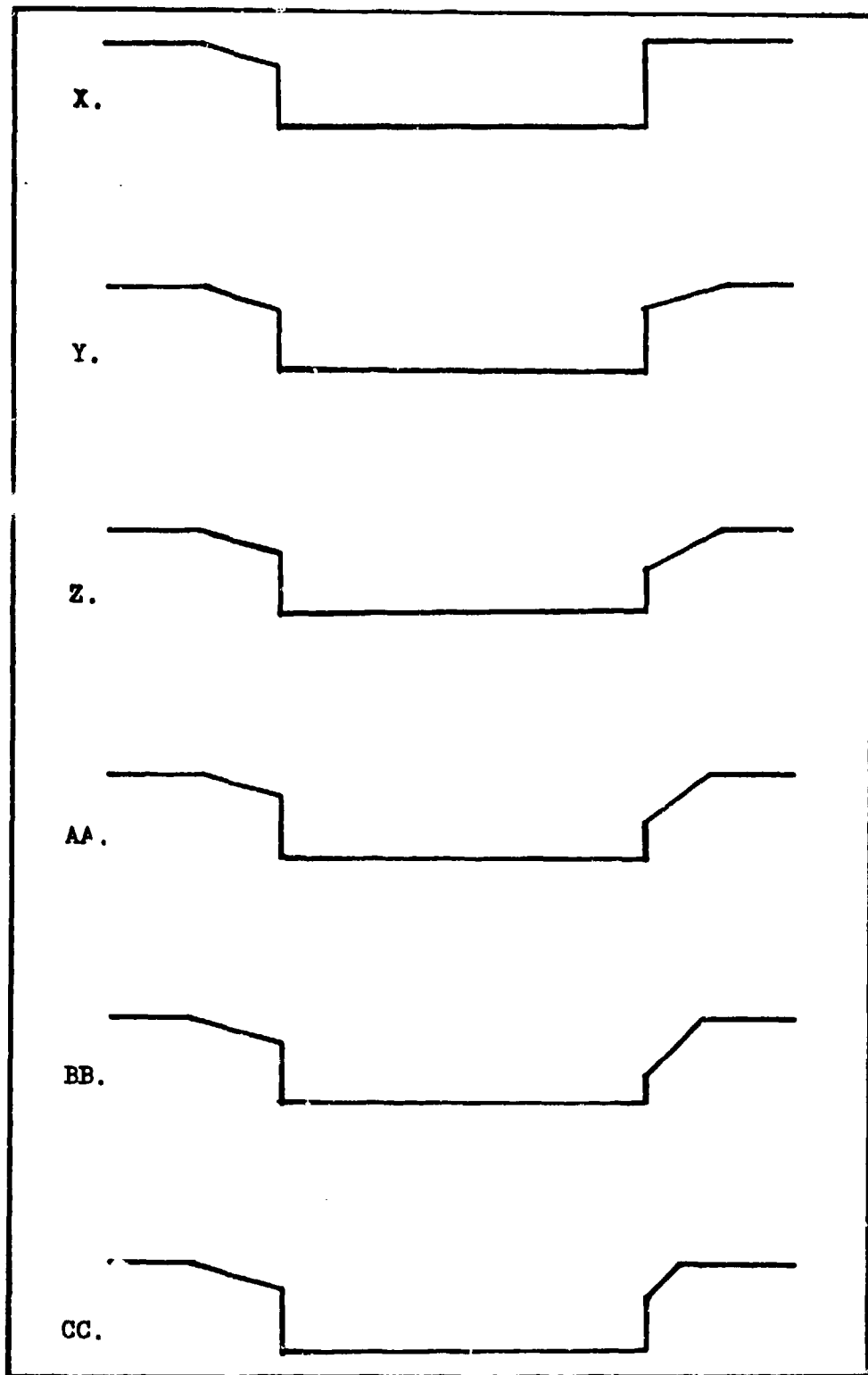


Fig. 8. $L/D = 4.25$ Cavity Configurations with 15 Degree, 1 Inch, Leading Edge Ramp.

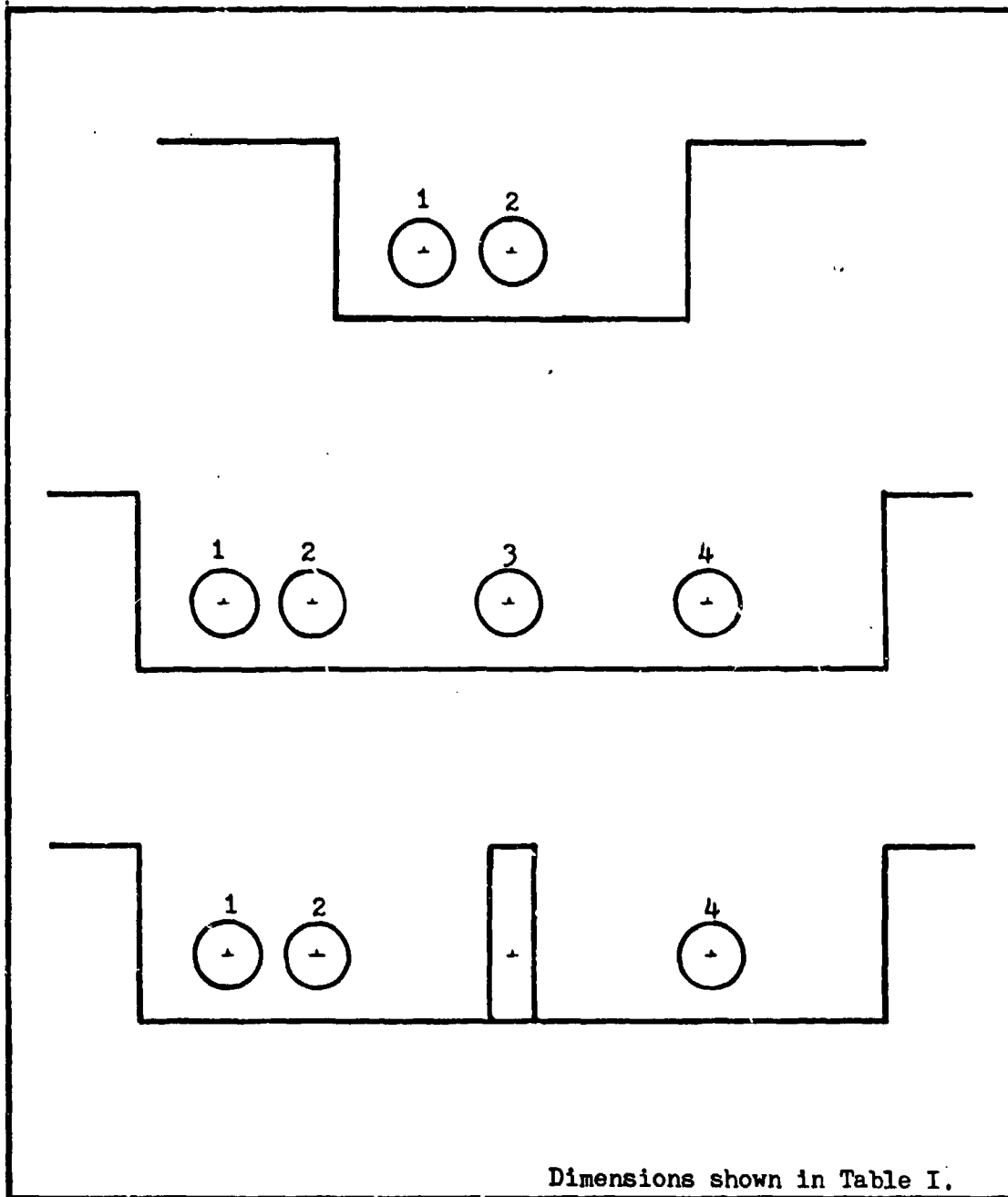


Fig. 9. Microphone Identities and Locations in Each Basic Cavity Configuration.

TABLE I.

Microphone Positions in Cavities (a)

Distance of microphones downstream from cavity leading edge are given in non-dimensional terms, X/L . (b)

<u>Cavity L/D</u>	<u>Microphone Number</u>	<u>Microphone Position, X/L</u>
(Single Cavities)		
2 (c)	1	0.25
	2	0.50
4.25	1	0.12
	2	0.24
	3	0.50
	4	0.76
(Double Cavity: Front)		
2	1	0.25
	2	0.50
(Double Cavity: Rear)		
2	4	0.50

-
- Notes: (a) Vertical position of all microphones is $3/8$ inch from cavity bottom. Configurations are shown in Fig. 9.
- (b) Center-line value; microphone sensor diameter is 0.25 inch.
- (c) Microphone number three is exposed to cavity trailing edge due to hole size although its centerline is beyond the trailing edge.

IV. Experimental Procedures

The microphones were calibrated before mounting them in the plexiglass panel. Each was mounted in an adapter which fitted in the driver cavity of a piston phone. The piston phone driver produced a 250 Hz signal at a nominal 124 dB sound pressure level. The signals of each microphone were recorded and later computer analyzed. The resulting amplitude vs frequency plots were compared to the known values to ensure that the equipment was functioning properly and that the correct procedures were being used.

To run a particular test, the desired cavity configuration and nozzle were fitted into the test section assembly. Using the appropriate fitting block constructed in the AFIT shop, the correct nozzle alignment (throat and exit dimensions) was set and all the assembly bolts were tightened. The assembly was bolted to the top of the calming chamber. The air flow was turned on and the delivery pressure was modulated until the nozzle exit static pressure was stabilized at atmospheric pressure as measured on a mercury manometer. When the system was stable, a one minute tape recording was made of the signals generated by the microphones. While the recording was being made, a schlieren photograph of the flow field in and above the cavity was made.

Cavity fluctuating pressure was sensed by four Model 376 Dynamic Pressure Transducers produced by Bolt, Beranek, and Newman, Inc. This information was recorded on an Ampex tape recorder at 30 in./sec. The frequency range capability of the recorder was 0-10 kHz. The recordings were processed through a Hewlett-Packard 5451B Fourier Analyzer at the Air Force Flight Dynamics Laboratory. The data were analyzed using 20 Hertz bandwidths to produce plots of sound pressure level amplitude

versus frequency for each microphone in the cavity.

A schlieren optical system with a spark lamp with a spark duration of $1/6$ microsecond was used to obtain still photographs of each test. Figure 10 is a schematic of the schlieren arrangement. The photographs were used to determine the Mach number of the flow over the cavity by measuring the Mach wave angle μ at the cavity leading edge and converting this to Mach number by the relation $M = 1/(\sin \mu)$. This value was used in the equations which predicted the frequencies of the possible response modes of the cavity.

During data collection using the $M = 1.20$ nozzle, it was determined that subsonic flow could be achieved and stabilized by opening a bleed valve on the air delivery system upstream of the test apparatus. This reduced the mass flow through the nozzle to a value below the amount required to achieve sonic flow at the nozzle throat. It was necessary to install an orifice meter in the air delivery pipe to determine the rate of flow. This data was used to compute the flow velocity at the nozzle exit. Data were collected at two subsonic flow conditions; one was the slowest velocity the apparatus would produce and the other was a higher setting (a particular pipe static pressure reading) at which a different cavity response could be audibly discerned.

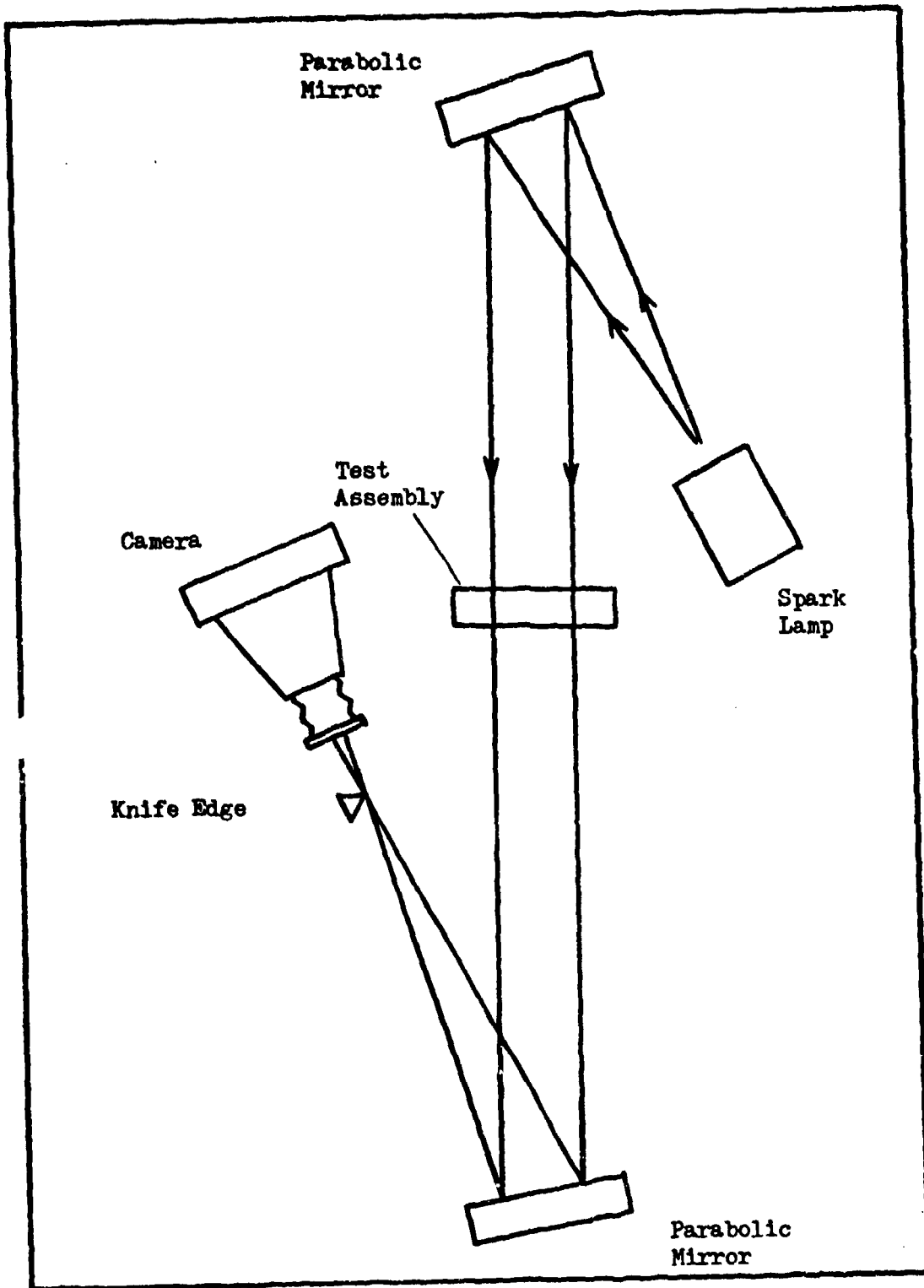


Fig. 10. Schematic of the Schlieren Apparatus.

V. Results and Discussion

Test Conditions

The three supersonic nozzles were designed assuming ideal flow and ignoring the boundary layer growth through the nozzle. Although the nozzle area ratio could be set to establish the design Mach number, it was expected that the actual conditions would differ. Table II lists the nozzle Mach numbers which were computed using the pressure data recorded for each run. Additionally, the flow Mach numbers determined from the wave angles at the cavity are listed.

It was found that the three nozzles produced Mach numbers at the cavity of approximately 1.5, 1.3, 1.0, 0.6, and 0.5. The subsonic values are based upon the assumption of a constant-pressure diffusion process downstream of the nozzle. Thus the Mach number and velocity decrease. The values chosen result from truncation of the nozzle values.

Resonant Frequencies

The resonant frequencies of the response of a cavity are identified by the dimensionless Strouhal number, $S = fL/U$.

Rossiter proposed the following empirical formula for the Strouhal number:

$$S = \frac{fL}{U} = \frac{m - 0.25}{M + 1.75} \quad (1)$$

where m is a positive integer and represents the frequency mode number. The model Rossiter used assumed the cavity temperature to be equal to the free stream static temperature (Ref 9:34).

Heller et al determined that the temperature in the cavity was closer to the free stream stagnation temperature (recovery factor closer

TABLE II

Mach and Reynolds Numbers Pertaining to the Test Assembly

<u>Nozzle Design</u> <u>Mach Nr</u>	<u>Measured Nozzle</u> <u>Mach Nr</u>	<u>Cavity</u> <u>Mach Nr</u>	<u>Reynolds</u> <u>Nr (a)</u>
1.61	1.58(b)	1.5(c)	4.65×10^6
1.39	1.36(b)	1.3(c)	3.30×10^6
1.20	1.06(b)	1.0(c)	2.32×10^6
----	0.68(d)	0.6(e)	1.53×10^6
----	0.59(d)	0.5(e)	1.16×10^6

- Notes: (a) Based on length from nozzle throat to cavity leading edge and isentropic values of density and velocity.
- (b) Ratio of exit static pressure (atmospheric) to total pressure (in calming chamber) was used to enter table in NACA Report 1135 to find nozzle exit Mach number for each run. Mean values listed.
- (c) Based on Mach wave angles.
- (d) Result of iteration procedure to compute a nozzle weight flow which was compared to the previously computed weight flow based on orifice meter data. Mean values listed.
- (e) Estimate based on constant pressure diffusion (deceleration) process downstream of nozzle.

to one than zero). They proposed a modified Rossiter formula for the Strouhal number which is:

$$S^* = \frac{fL}{U} = \frac{m - 0.25}{\frac{M}{(1 + .2M^2)^{1/2}} + 1.75} \quad (2)$$

This formula was shown to provide better correlation of the discrete-frequency response of the cavity primarily for Mach numbers above 0.5 (Ref 9:35). The formula does not predict that a response frequency will exist. The formula was considered to be most applicable to shallow cavities, where L/D is 4 or greater, and the accuracy was estimated to be ± 10 per cent (Ref 9:96).

The resonant frequencies and corresponding Strouhal numbers present in the cavities in this study are shown along with the expected results according to Eq(2), in Tables III and IV. The Strouhal numbers for this study are shown in Figs. 11 and 12 with previous data and the Rossiter formulas.

Mach Number Effect on Fluctuating Pressure Levels

Plots of resonant frequency fluctuating pressure amplitudes against Mach number are given in Figs. 13 through 19. The data represent the maximum levels found on pertinent plots of amplitude vs frequency. Figure 13 shows the maximum Sound Pressure Level (SPL) measured by any microphone in any mode in the $L/D = 2$ cavities. For each cavity shape ($L/D = 2$) for which data were collected at all Mach numbers, the maximum levels occur for sonic velocity over the cavity and drop off with increasing or decreasing Mach numbers. This is representative of results presented by Heller et al (Ref 5:96, 105-116) where the relative maximum occurred at transonic speeds (generally $M = 1.2$). Figure 14 shows that

the maximum levels for the $L/D = 4 \frac{1}{4}$ cavities occur at $M = 1.3$. Although the data are not as orderly as in Fig. 13, there appears to be a trend for the level to decrease as the flow velocity increases above the transonic.

Suppression Effectiveness on Fluctuating Pressure Levels

The relative suppression effectiveness of ramps on the leading and trailing edge of the cavities is represented in Fig. 13 and Fig. 14.

$L/D = 2$ Cavities. In Fig. 13 the various trailing edge ramps are shown to lower the resonant levels relative to the straight trailing edge. For the straight leading edge, the $\frac{1}{2}$ inch, 45° , rear ramp provides suppression up to 6 dB and the 25° , 1 inch, ramp produces a 14 dB suppression relative to the rectangular cavity. For the two Mach numbers tested, the 45° , 1 inch, ramp suppressed resonance up to 26 dB. The leading edge ramp showed suppression effects generally between those of the 25° and 45° 1 inch rear ramps.

The relative effectiveness of the one inch trailing edge ramps to suppress the resonant cavity response followed the pattern predicted by previous investigations (Ref 5, Ref 7). Increasing the ramp angle increased the suppression in the cavity. The $\frac{1}{2}$ inch, 45° , ramp created significantly less oscillation suppression than all the one inch long ramps except the 15° ramp. Since the intended purpose of the trailing edge ramps was to prevent the mass-exchange process, the short ramp was apparently not able to stabilize the stagnation point of the shear layer. This presumed inability is most likely due to the size of the ramp relative to the thickness of the shear layer at that point. In the schlieren photographs, the shear layer thickness is approximately

TABLE III

Resonant Frequency Data for the L/D = 2 Rectangular Cavity

M	n	f,exp	S,exp	f,Eq(2)	S*,Eq(2)	Difference in %
0.5	1	----	----	1122	0.34	-----
	2	1725	0.52	2574	0.78	-33.3
	3	3668	1.11	4059	1.23	-9.8
	4	5423	1.64	5544	1.68	-2.4
	5	7143	2.16	6996	2.12	+1.9
0.6	1	830	0.21	1248	0.32	-34.4
	2	2053	0.53	2925	0.75	-29.3
	3	4064	1.04	4602	1.18	-11.9
	4	6237	1.60	6279	1.61	-0.6
	5	8303	2.13	7956	2.04	+4.4
1.0	1	2100	0.34	1730	0.28	+21.4
	2	4253	0.69	4079	0.66	+4.5
	3	6383	1.03	6365	1.03	0.0
	4	8425	1.36	8714	1.41	-3.5
1.3	1	2208	0.29	1980	0.26	+11.5
	2	4417	0.58	4645	0.61	-4.9
	3	7208	0.95	7309	0.96	-1.0
	4	9452	1.24	9898	1.30	-4.6
1.5	1	----	----	2111	0.25	----
	2	5221	0.62	4896	0.58	+6.9
	3	8372	0.99	7767	0.92	+7.6

TABLE IV

Resonant Frequency Data for the L/D = 4.25 Rectangular Cavity

M	n	f,exp	S,exp	f,Eq(2)	S*,Eq(2)	Difference in %
0.5	1	789	0.51	528	0.34	+50.0
	2	1474	0.95	1211	0.78	+21.8
	3	2199	1.42	1910	1.23	+15.4
0.6	1	856	0.47	587	0.32	+46.9
	2	1711	0.93	1376	0.75	+24.0
	3	2718	1.48	2166	1.18	+25.4
	4	3428	1.87	2955	1.61	+16.1
	5	4456	2.43	3744	2.04	+19.1
1.0	1	707	0.24	814	0.28	-14.3
	2	2173	0.75	1919	0.66	+13.6
	3	2832	0.97	2995	1.03	-5.8
	4	3439	1.18	4101	1.41	-16.3
1.3	1	757	0.21	932	0.26	-19.2
	2	2289	0.64	2186	0.61	+4.9
	3	3809	1.06	3440	0.96	+10.4
	4	4542	1.27	4658	1.30	-2.3
1.5	1	799	0.20	993	0.25	-20.0
	2	2327	0.59	2304	0.58	+1.7
	3	3858	0.97	3635	0.92	+5.4
	4	4673	1.18	4966	1.25	-5.6
	5	6283	1.58	6317	1.59	-6.3

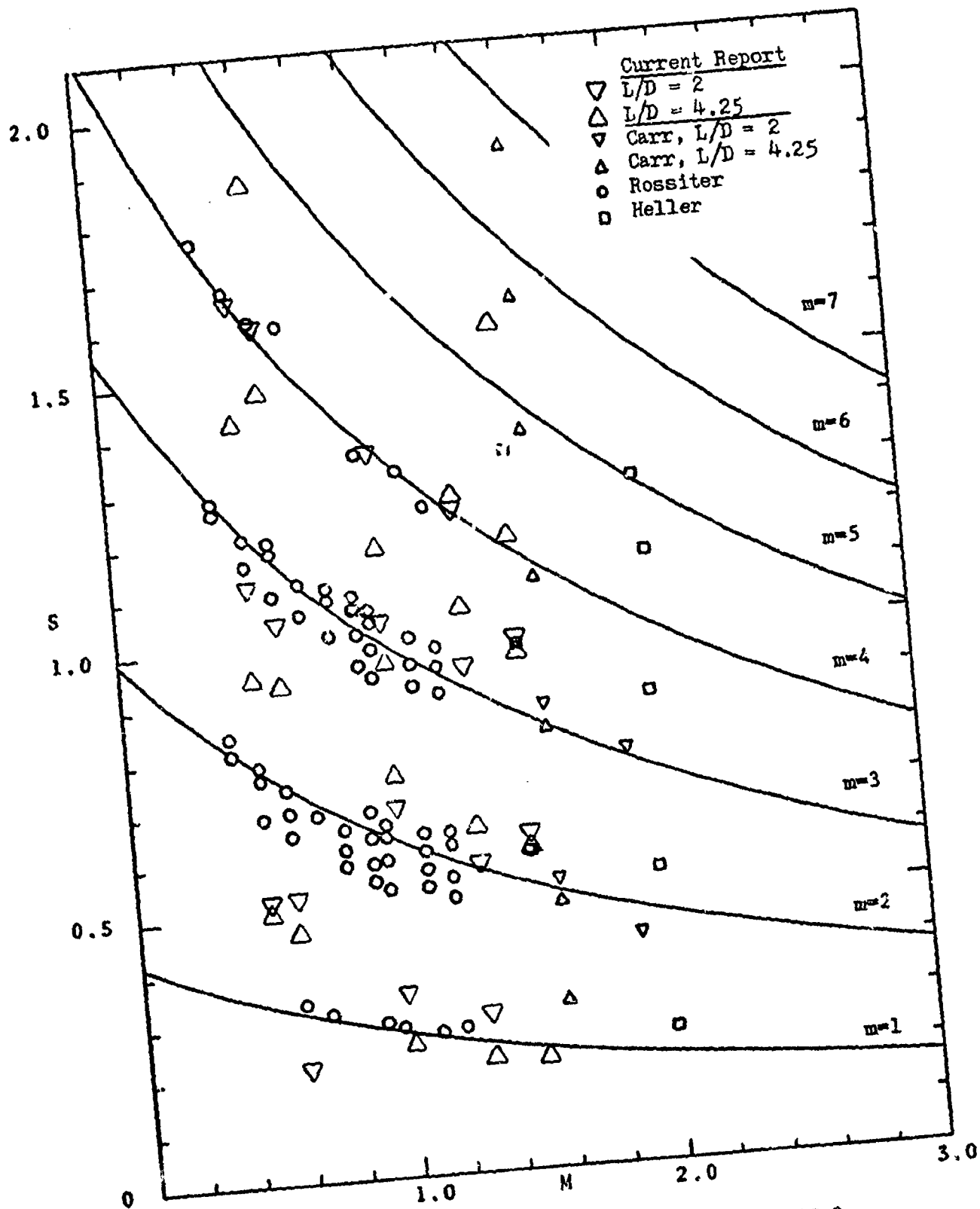


Fig. 11. Nondimensional Resonant Frequencies as a Function of Mach Number with Implementation of Rossiter's Formula.

Source: Carr (Ref 7)

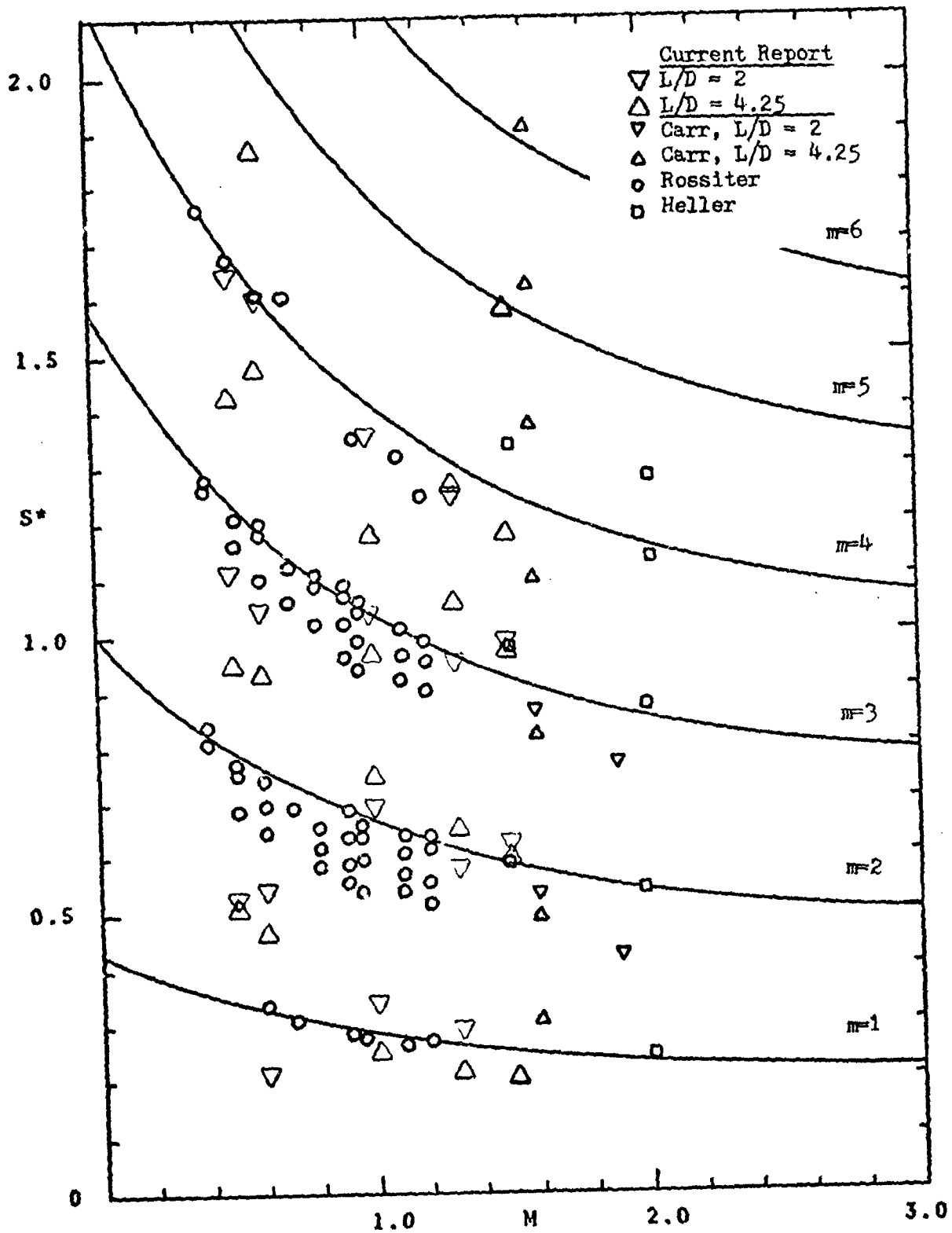


Fig. 12. Nondimensional Resonant Frequencies as a Function of Mach Number with Implementation of Modified Rossiter Formula.

Source: Carr (Ref 7)

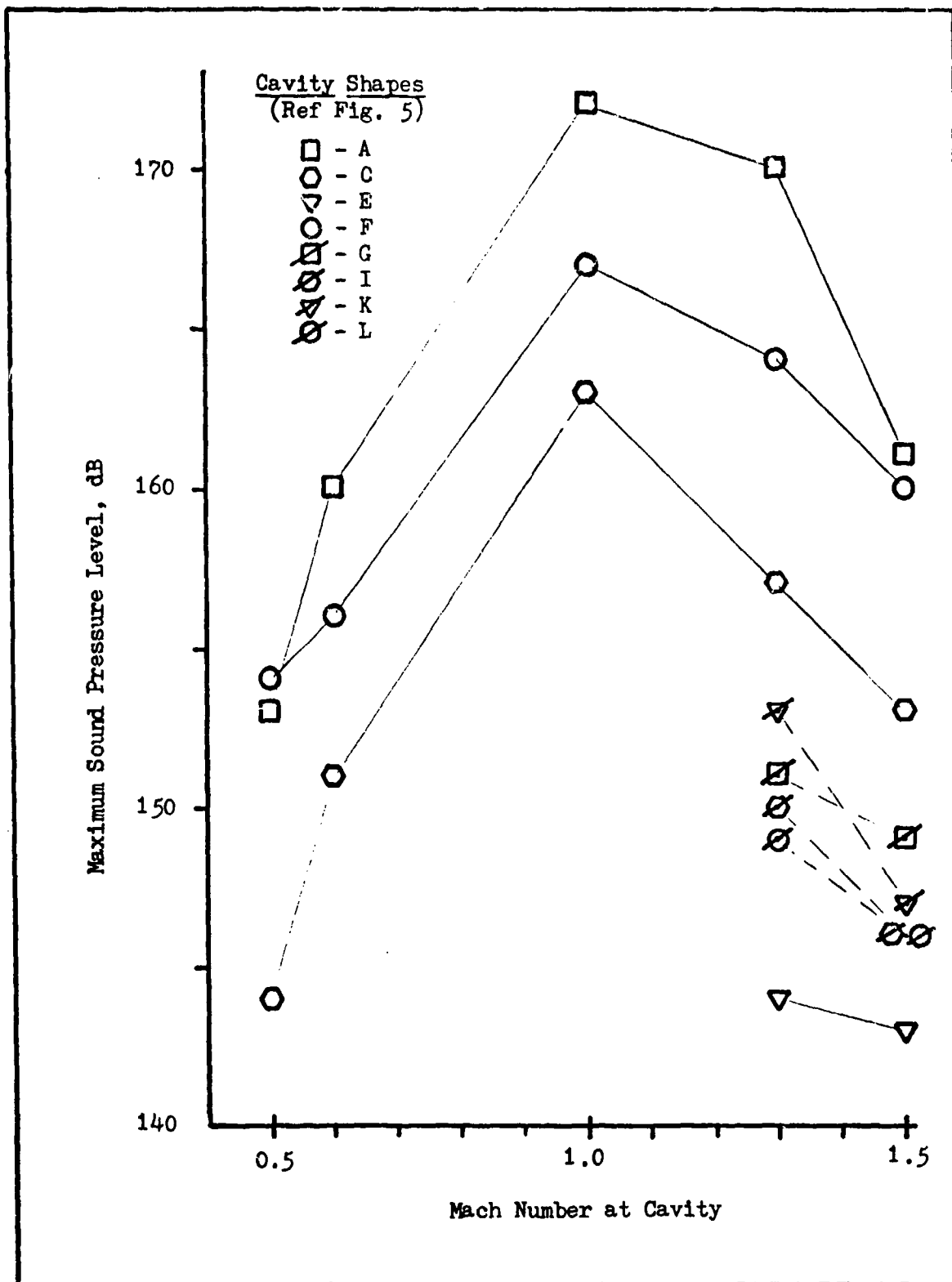


Fig. 13. Maximum Dynamic Pressure Amplitude Variation with Mach Number for $L/D = 2$ Cavities.

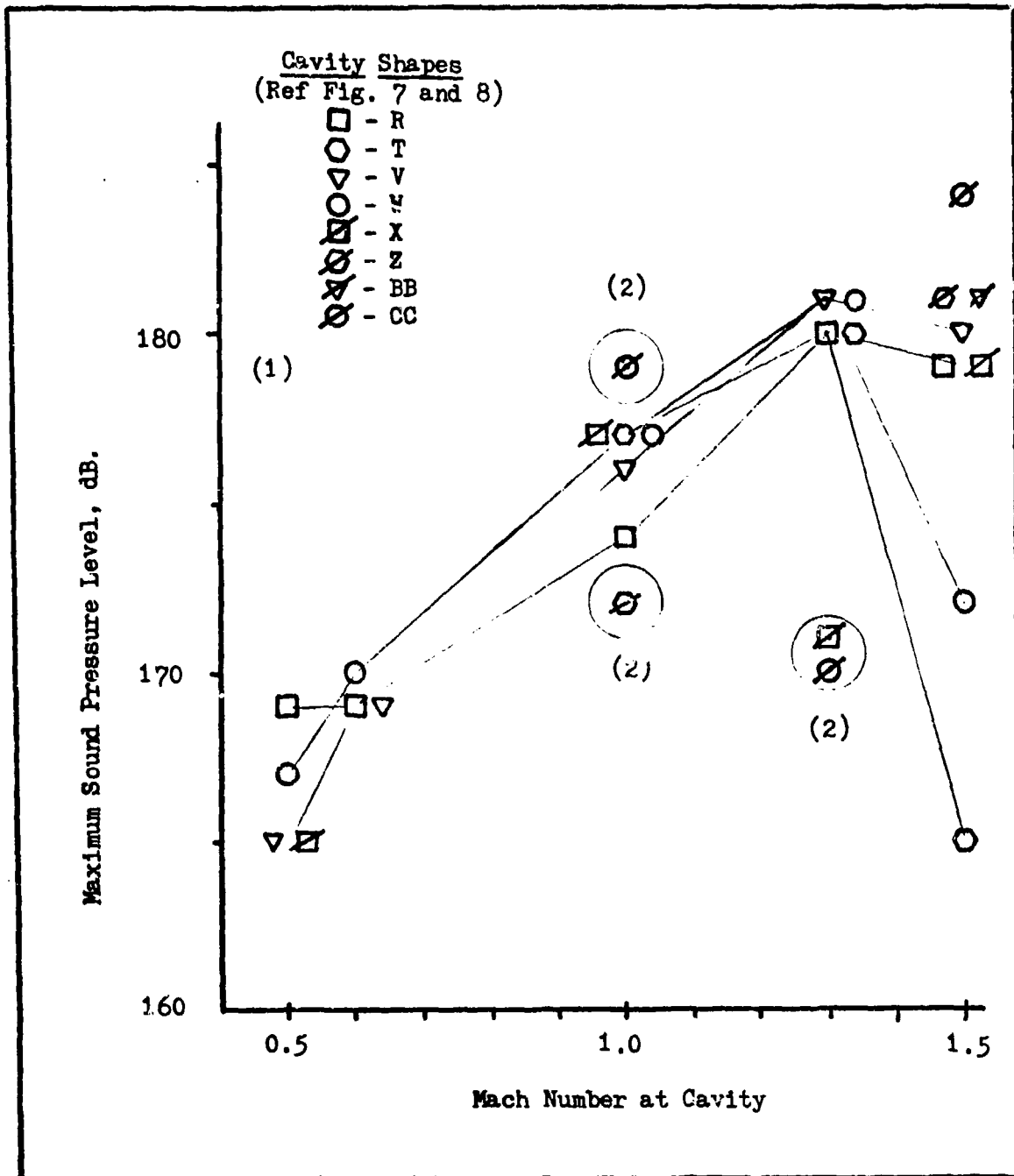


Fig. 14. Maximum Dynamic Pressure Amplitude Variation with Mach Number for $L/D = 4.25$ Cavities.

- Notes: (1) Plots on which amplitude is 179 dB or greater indicate the microphones were swamped; the true amplitude may be greater.
- (2) Data pertains to unswamped microphones; plots for swamped microphones were not generated.

the size of the projected vertical dimension of the ramp. The relative sizes and the vertical oscillations of the shear layer are probably the principal reasons the stagnation point was not stable and the suppression effectiveness was reduced.

L/D = 4 1/4 Cavities. The results of tests on the L/D = 4 1/4 cavities are shown in Fig. 14. In many cases the SPL exceeded the upper limit of the microphones. Results involving swamped microphones can only be discussed qualitatively. The response of all the cavities with the leading edge ramps swamped at least one of the microphones in each test. In general, the leading edge ramp had an amplifying effect on the L/D = 4 1/4 cavity response. The effects of the trailing edge ramps are not consistent. At a Mach number of 1.5 the 25° ramp demonstrated a 14 dB reduction, the 45°, 1/2 inch, ramp a 7 dB reduction, but the 45°, 1 inch, ramp raised the response by 1 dB. At the Mach number of 1.3 the levels differ only by 1 dB. At sonic velocity the trailing edge ramps raised the response of the cavity by 2 or 3 dB above the rectangular cavity response. At the subsonic conditions the relative effects reversed again; at the Mach number of 0.5 the rectangular cavity produced the greatest response by 2 to 4 dB.

Certain characteristics of the flow across the cavities with a leading edge ramp were evident in the schlieren photographs. In all cases the flow remained attached at the forward end of the ramp, i. e., the flow turned down 15° and followed the ramp. However, in all cases the flow separated after traversing 1/4 to 1/3 of the ramp length. The shear layer which developed at the separation point appeared to be several times thicker than a shear layer at a straight leading edge. The shear layer may also have been more unstable than a shear layer initiated at

the straight leading edge. This can not be conclusively determined from the photographs. One or more of the shear layer characteristics probably contributed to the amplification phenomena associated with the leading edge ramp: shear layer lower in the cavity, thicker, and probably more turbulent or unstable.

Modes of Fluctuating Pressure Levels

More complete plots of the maximum sound pressure levels in the cavities are presented in Figs. 15 through 19. Each spectra plot of SPL versus frequency was used to give a mode-1 and a mode-2 data point on the appropriate figure. In the 2 inch cavity the mode-1 response did not exist at Mach number 1.5, but it was the significant mode at lower velocities (Fig. 15, 16, 17). These two features are contrary to recent large-scale wind tunnel test results (Ref 5:96). An additional feature of the plots is that microphone number one generally sensed greater levels than number two; although, the background noise levels were generally higher on microphone number two. Larger scale tests produced an opposite trend (Ref 9:72), i.e., maximum and background levels were greater near the cavity trailing edge.

Because the maximum levels in this study usually occurred on microphone number 1, the upper and lower values of microphone number 1 data for the $4\frac{1}{4}$ inch cavity were connected in Fig. 18 to represent the differences of SPL between duplicate test runs of a cavity shape. The method used to analyze the microphone signals can introduce a three dB variation in the plotted maximum SPL. This variation would depend on the position of the frequency of the pure tone within the 20 Hz bandwidth used to analyze it. Only mode-1 data is plotted in Fig. 19. Higher mode

tones and higher frequency tones not associated with modes of resonance were present on the plots. Their levels were lower than the mode-1 levels by as much as 20 dB.

Narrow-band Spectra of Fluctuating Pressure Levels

L/D = 2 Cavities. Representative plots of sound pressure levels in the short cavities are presented in Figs. 20 through 25. Figure 20 and Fig. 21 show the response of the short rectangular cavity at each of the five test conditions. At sonic velocity the plot indicates there are more tones in the cavity response than at other velocities. Not all of the tones can be associated with modes. The difference between the maximum tone levels and the background levels of the sonic and supersonic velocity plots are similar. The second tone of the sonic velocity spectra has the maximum level. This tone has been identified as the mode-1 response since its frequency is closer to the mode-1 frequency predicted by the modified Rossiter formula. On this basis, the results of this investigation differ from that of Heller (Ref 5) where the mode-2 has the maximum amplitudes. Another general characteristic evident in Fig. 20 is that the broadband levels are greater by up to 10 dB on microphone number 2 plots. Thus the broadband levels are apparently greater in the trailing edge region than in the leading edge region. This is consistent with the findings of Heller (Ref 5:101). According to the plots in Fig. 21, a decreasing subsonic Mach number caused the discrete frequency levels to reduce in conjunction with the broadband reductions.

Figures 22, 23, and 24 show the effects of the selected trailing edge ramps on the cavity spectra. The effects on the maximum sound pressure levels were discussed previously. In general the ramps reduced

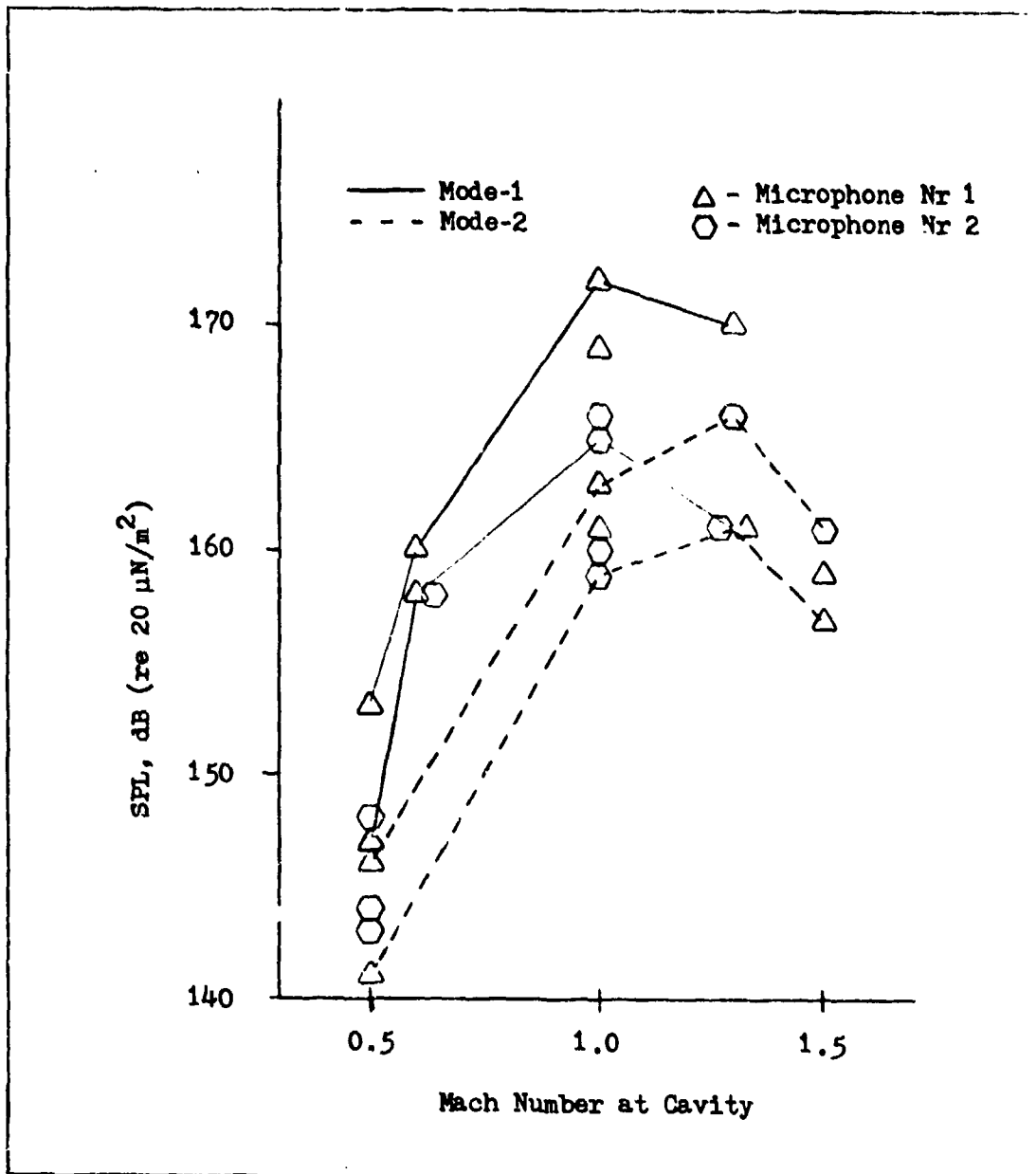


Fig. 15. Range of Maximum Sound Pressure Levels in the Rectangular $L/D = 2$ Cavity as a Function of Mach Number.

Lines drawn through maximum and minimum values independent of microphone position.

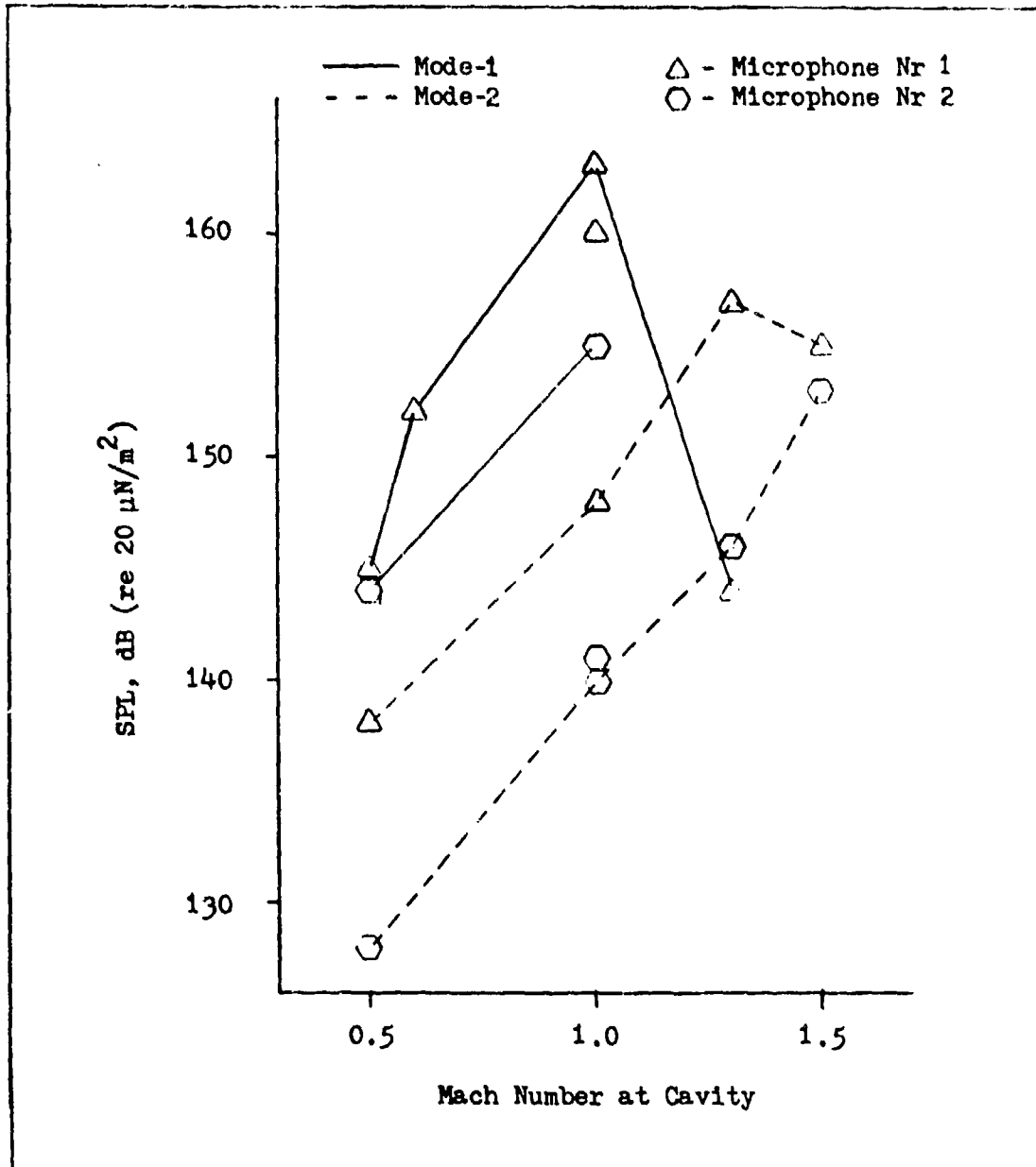


Fig. 16. Range of Maximum Sound Pressure Levels in the $L/D = 2$ Cavity with 25° , 1 inch, Trailing Edge Ramp as a Function of Mach Number.

Lines drawn through maximum and minimum values independent of microphone position.

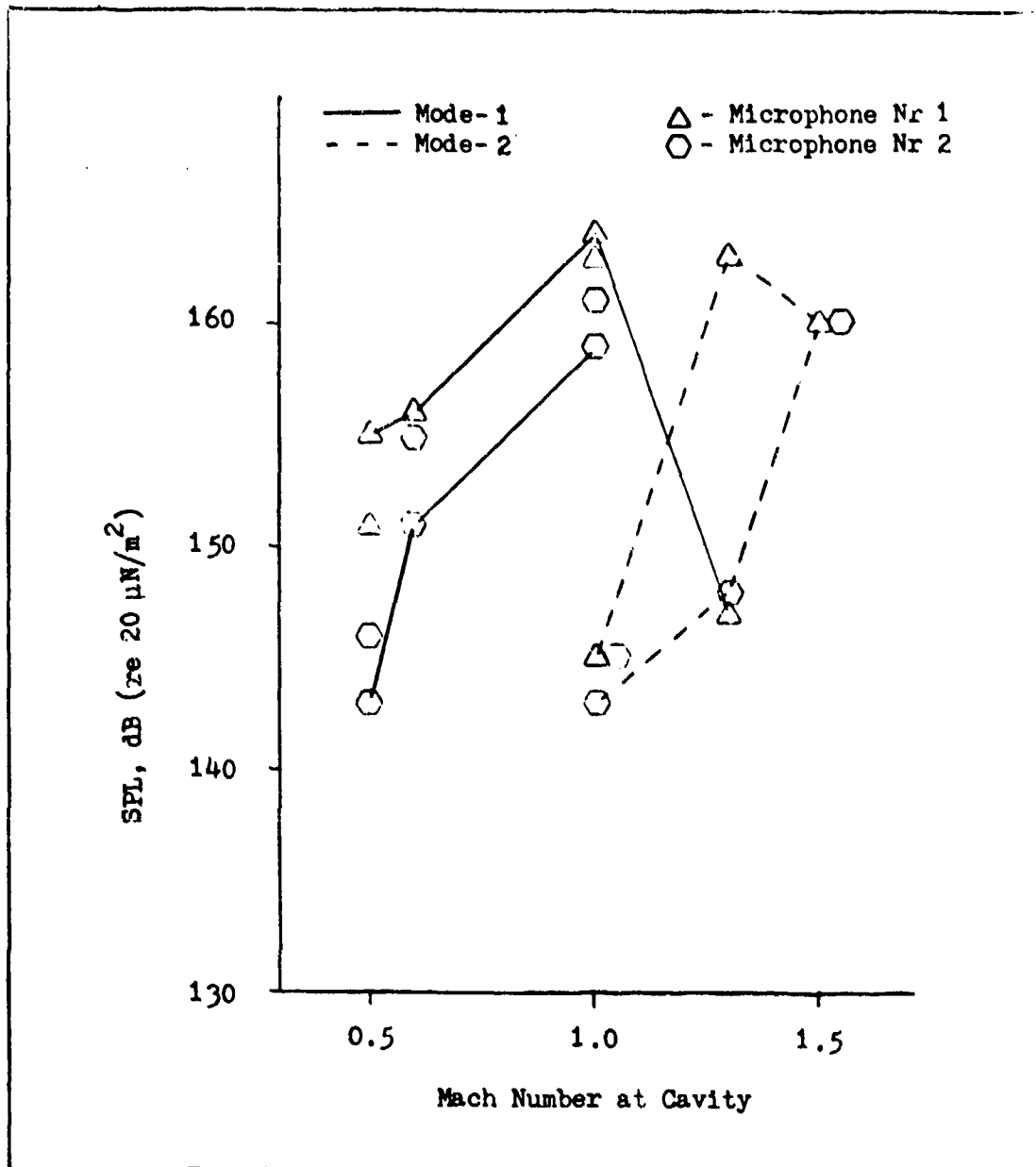


Fig. 17. Range of Maximum Sound Pressure Levels in the $L/D = 2$ Cavity with 45° , 1/2 inch, Trailing Edge Ramp as a Function of Mach Number.

Lines drawn through maximum and minimum values independent of microphone position.

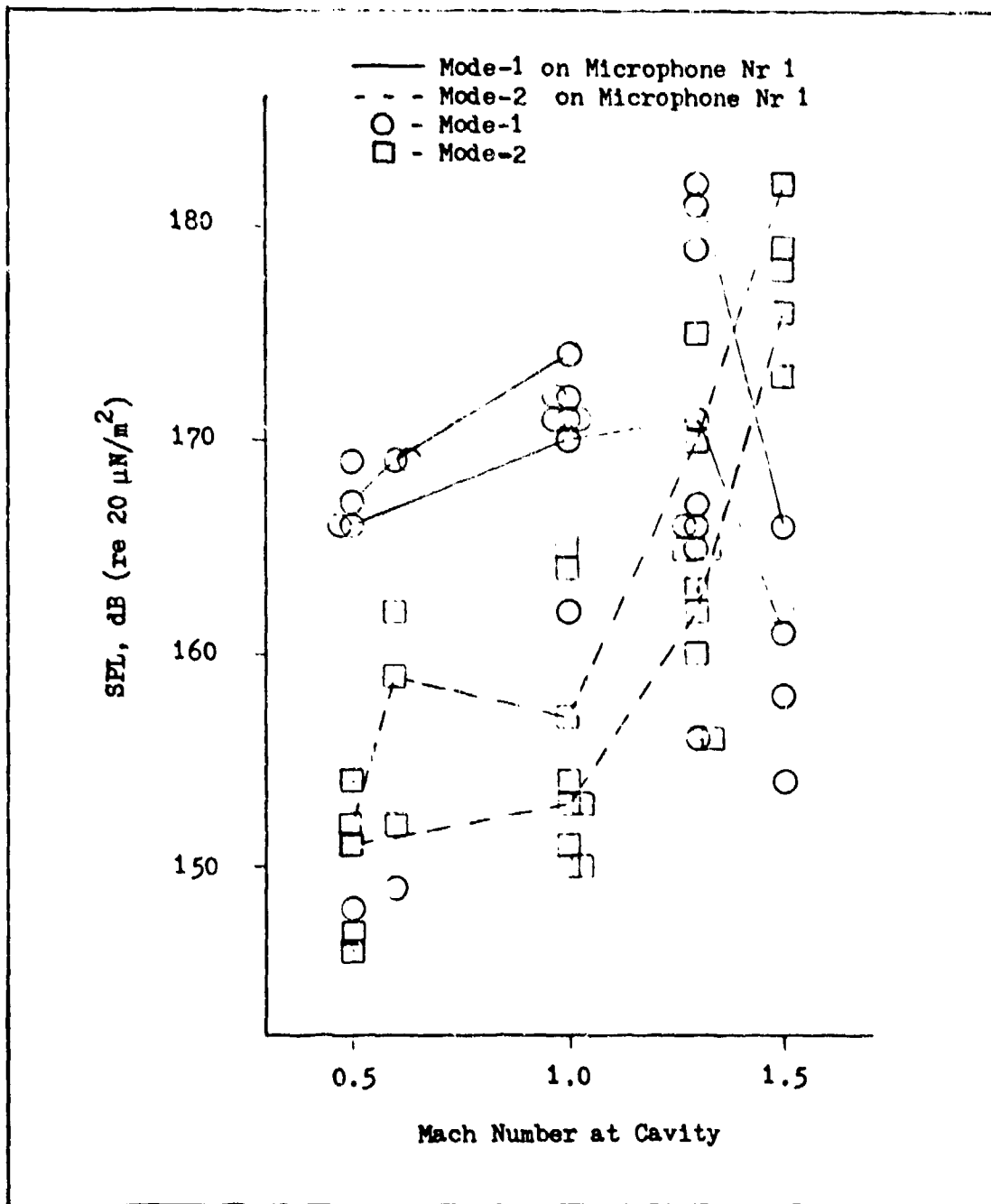


Fig. 18. Range of Maximum Sound Pressure Levels in the $L/D = 4.25$ Rectangular Cavity as a Function of Mach Number.

Lines drawn through maximum and minimum values of microphone nr 1 data for each mode.

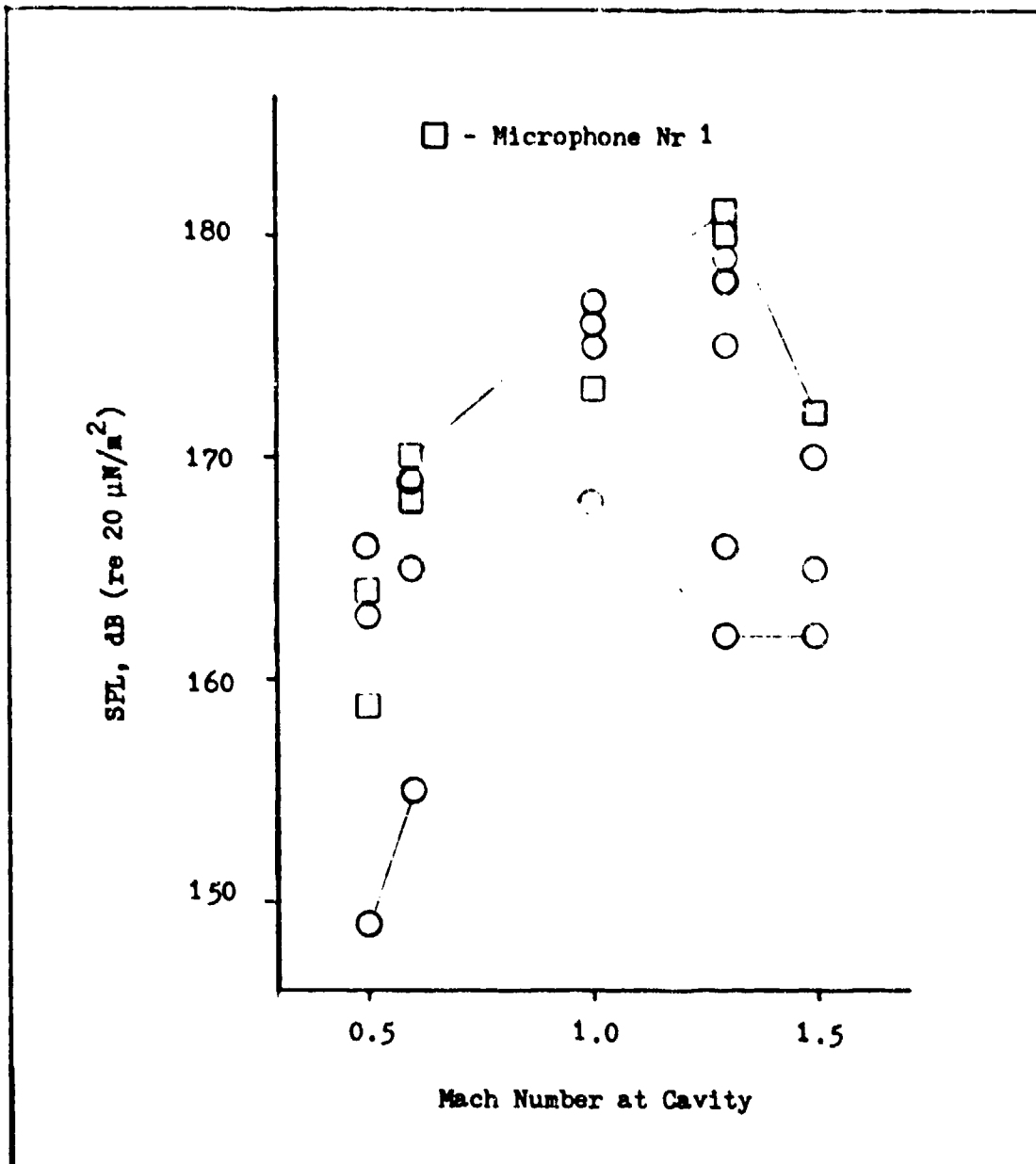


Fig. 19. Range of Mode-1 Sound Pressure Levels in the $L/D = 4.25$ Cavity with 45° , 1 inch, Trailing Edge Ramp.

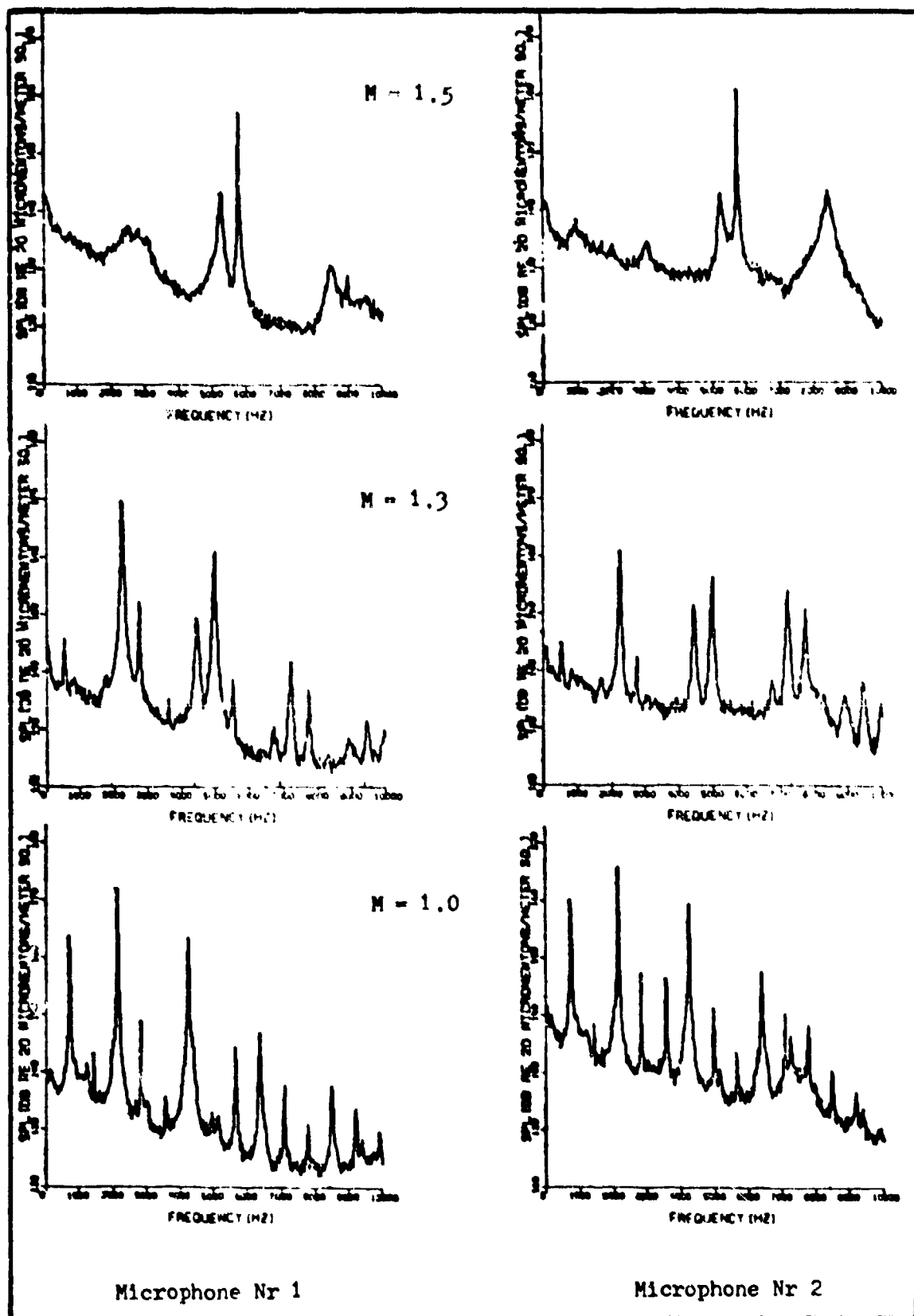


Fig. 20. Sound Pressure Level (SPL) Variation with Frequency in the $L/D = 2$ Rectangular Cavity at $M = 1.5, 1.3,$ and 1.0 .

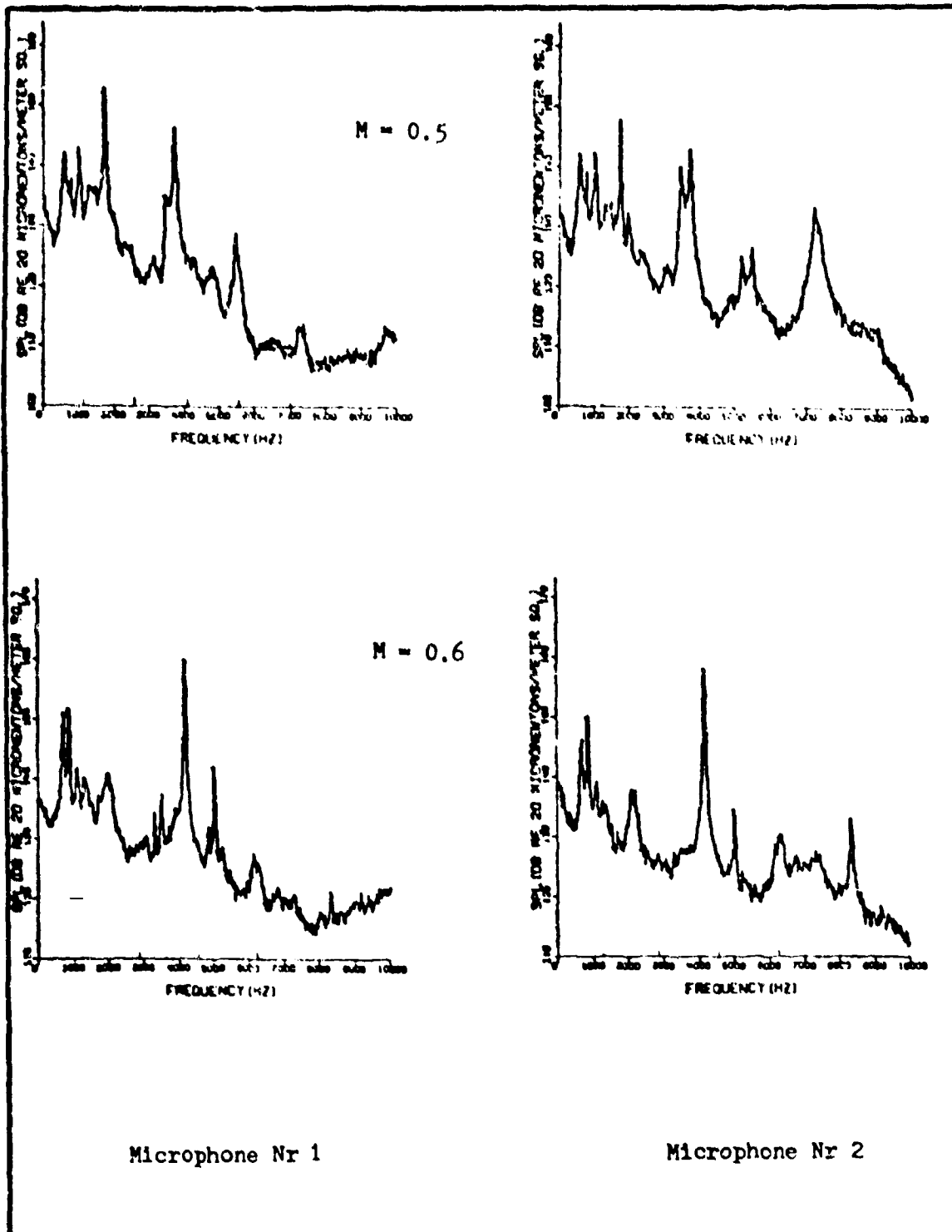


Fig. 21. Sound Pressure Level Variation with Frequency in the $L/D = 2$ Rectangular Cavity at $M = 0.6$, and 0.5

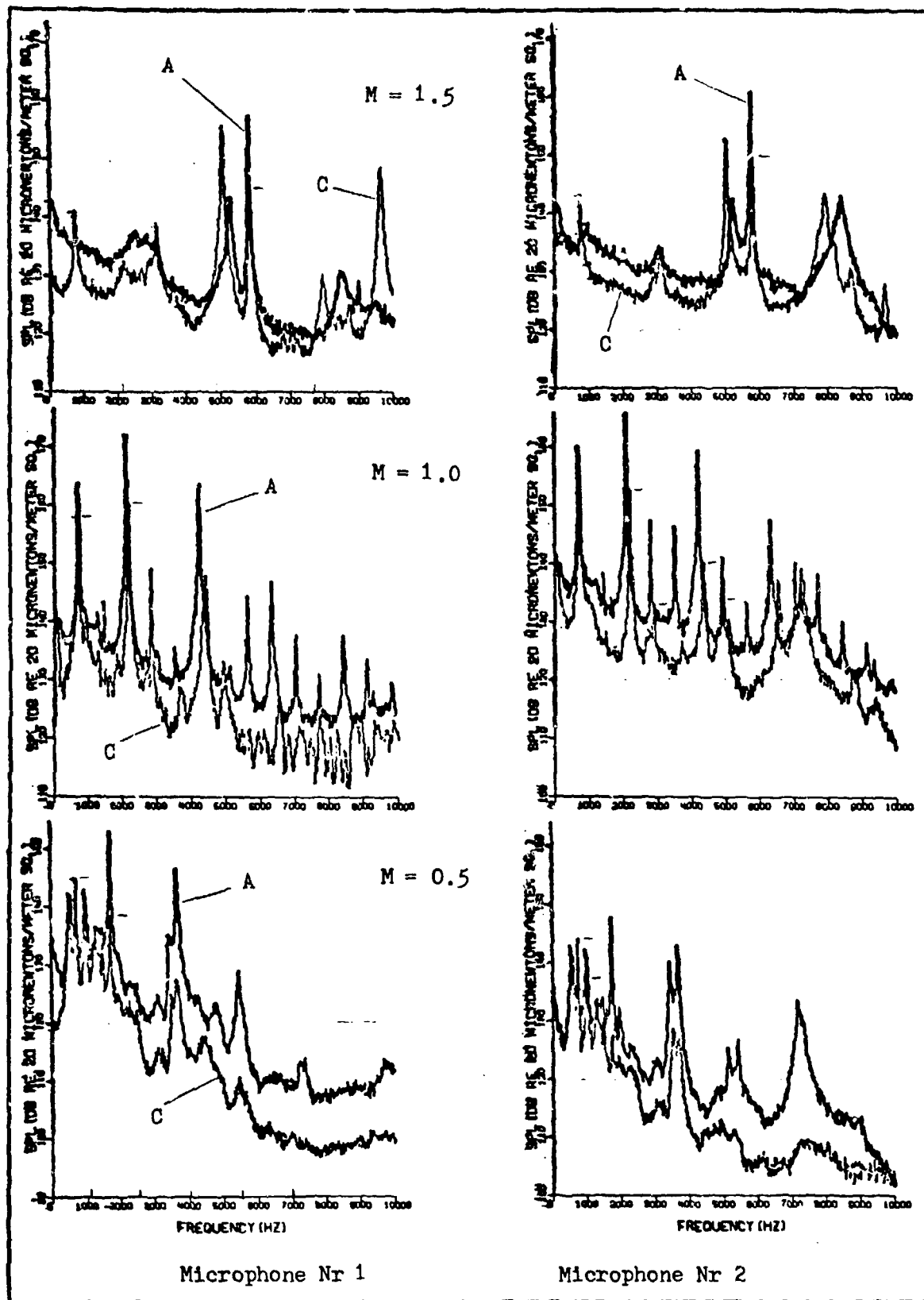


Fig. 22. Comparison of L/D = 2 Rectangular (A) and 25° Rear Ramp (C) Cavity SFL at M = 1.5, 1.0, and 0.5.

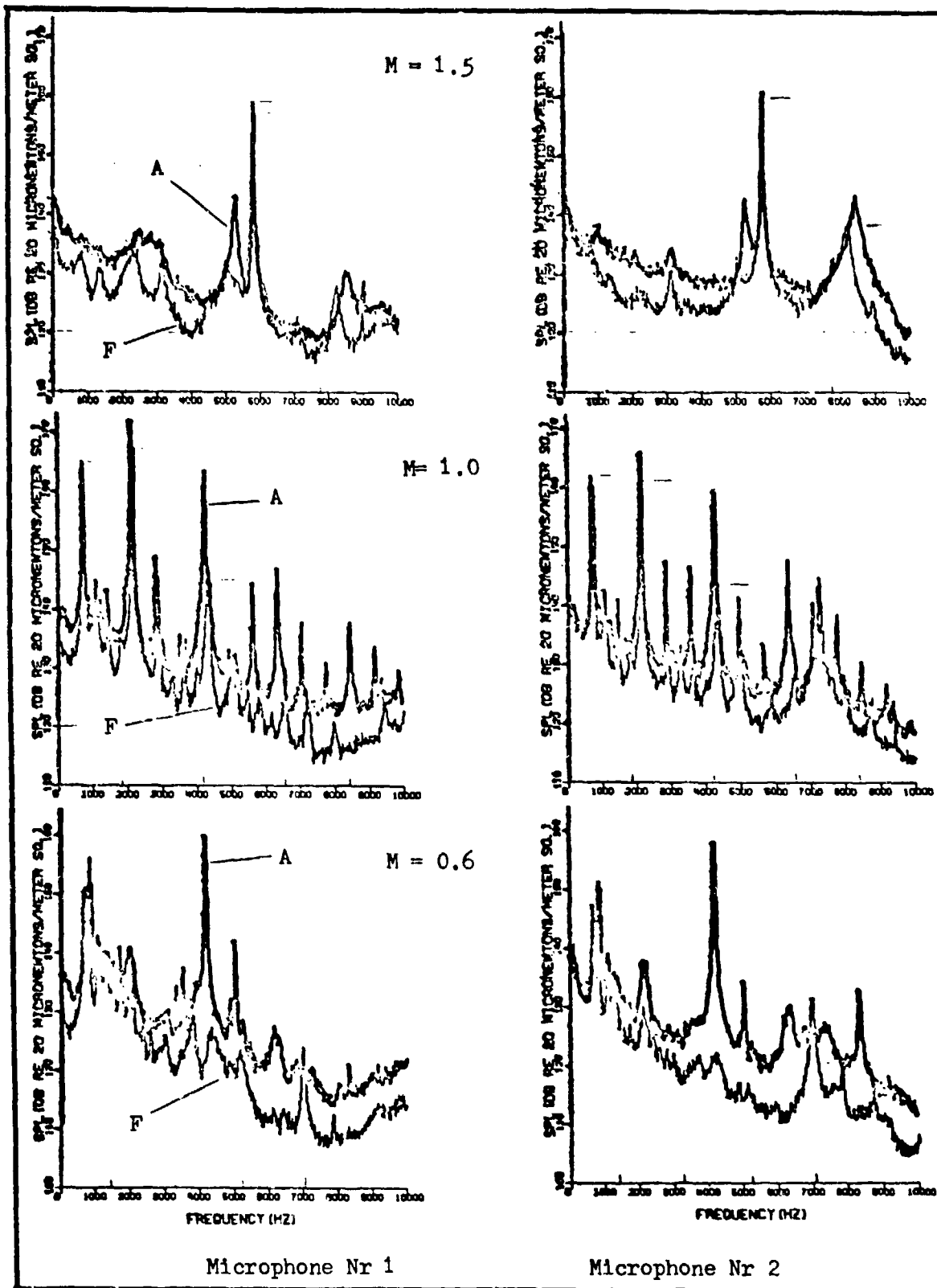


Fig. 23. Comparison of $L/D = 2$ Rectangular (A) and 45° , $1/2$ Inch, Rear Ramp (F) Cavity SPL at $M = 1.5, 1.0, \text{ and } 0.6$.

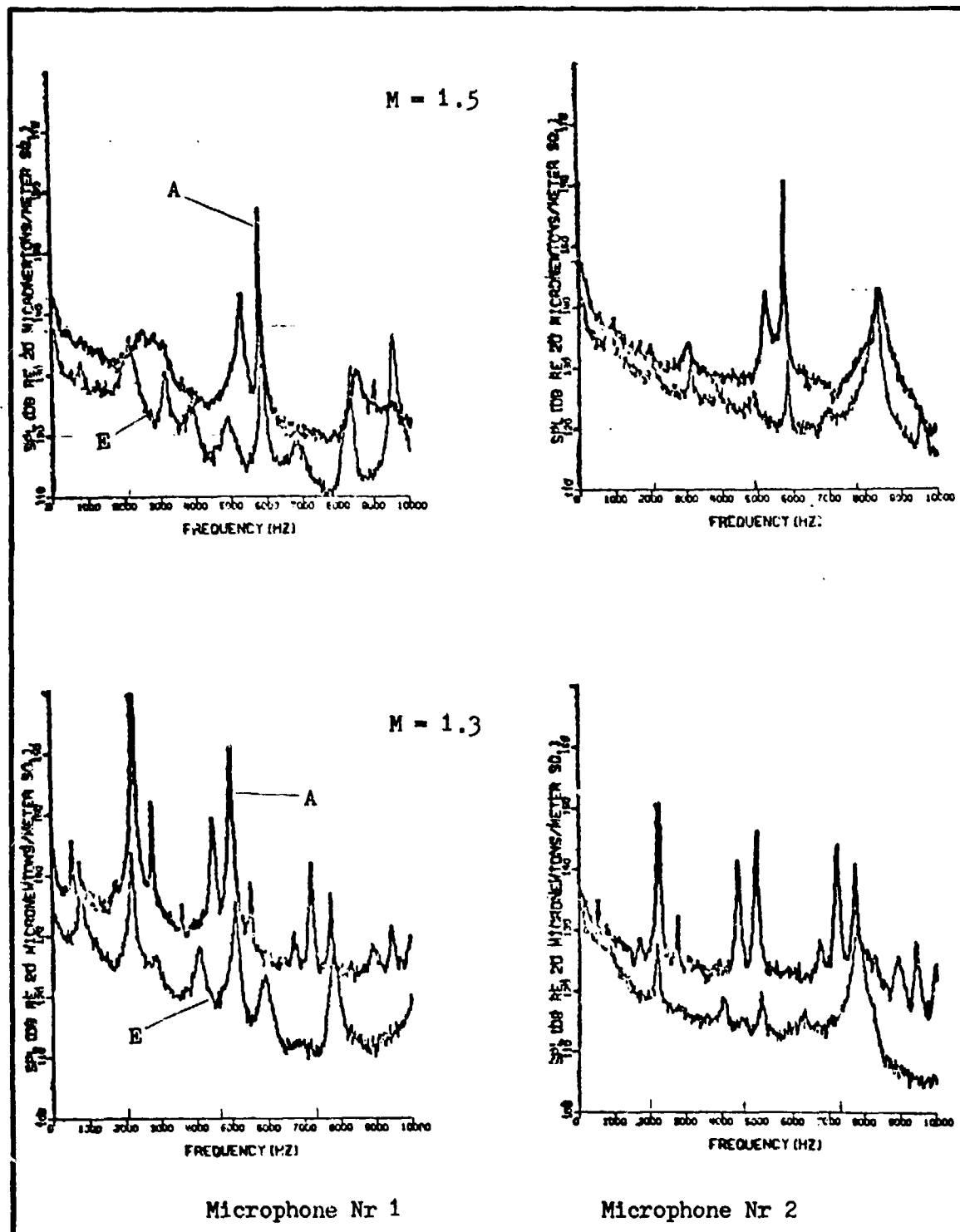


Fig. 24. Comparison of $L/D = 2$ Rectangular (A) and 45° , 1 Inch, Rear Ramp (E) Cavity SPL at $M = 1.5$ and 1.3 .

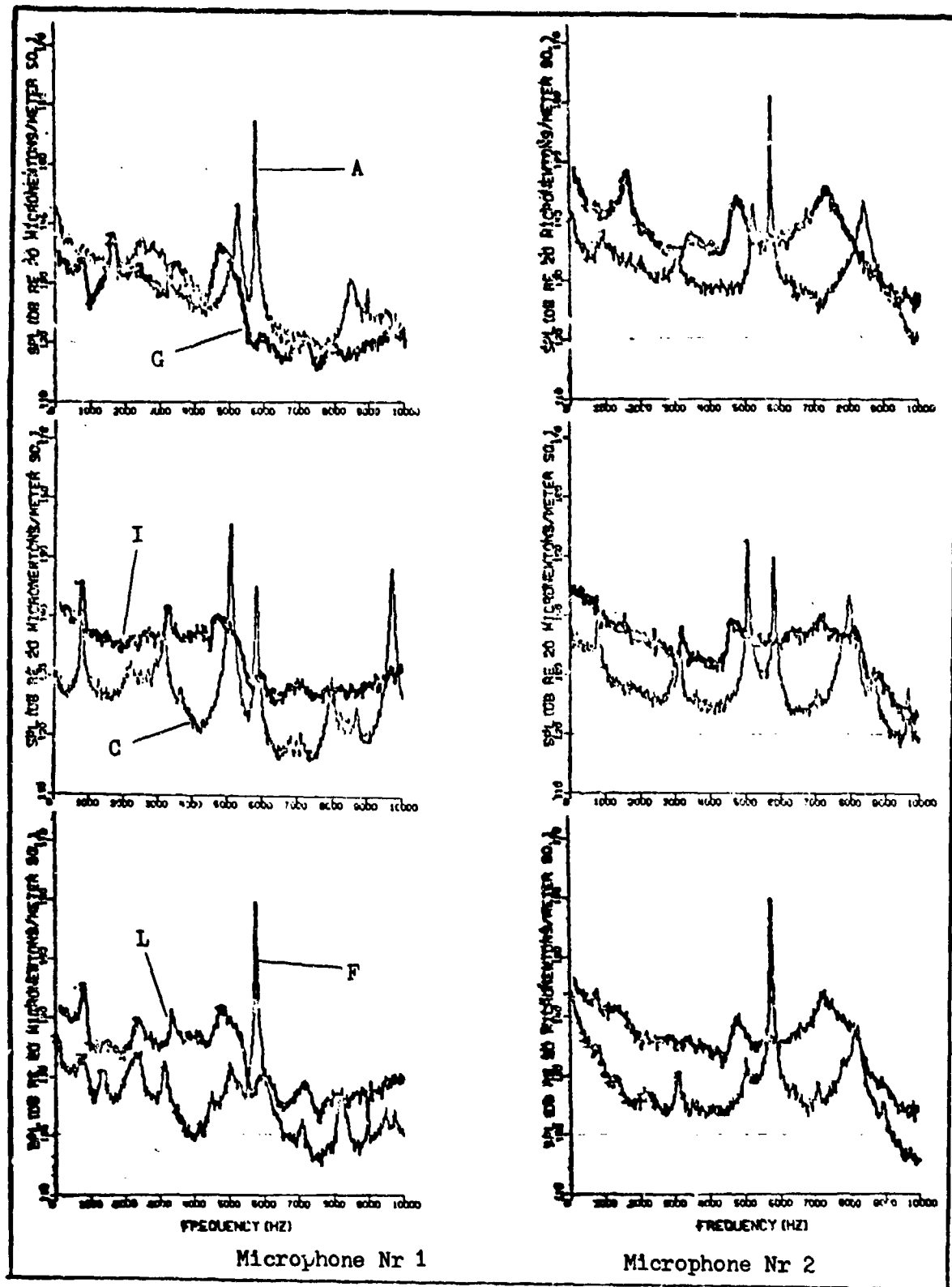


Fig. 25. Comparison of SPL in $L/D = 2$ Cavities with and without Leading Edge Ramp at $M = 1.5$.

See Fig. 5 for Cavity Shape Identification.

discrete frequency and broadband levels. One significant exception is the effect of the 25° ramp at $M = 1.5$ (C in Fig. 22). Microphone Nr 1 detected a mode-4 response which did not exist in the rectangular cavity. Similarly the 45° , 1 inch, ramp magnified the mode-3 response relative to the broadband level (see Fig. 24) and also apparently caused a mode-4 response to develop.

The effect of the leading edge ramp is shown in Fig. 25. The ramp eliminated all discrete frequency responses and generally raised the broadband levels. Thus the leading edge ramp was much more successful at reducing the cavity resonance than the trailing edge ramps.

Tandem $L/D = 2$ Cavities. It was determined that the front cavity pressure fluctuations were similar to those in the single cavity with identical configuration and flow conditions. In some cases the SPL plots were exact duplicates. Minor differences did appear at some flow conditions. For example, at $M = 1.0$, the front cavity response did not contain the lower level modes which were found for the single cavity. It was found that the rear cavity responded in a manner similar to the front regardless of the shape of the trailing edge. For example, in the configuration with a front rectangular cavity and a rear cavity with a trailing edge ramp, the spectra of the rear cavity is nearly identical to that of the front cavity and does not exhibit any similarity to the response of the single cavity with the same shape. Thus the shape of the trailing edge has almost no suppression effect on tandem cavity response. The suppression effectiveness of the leading edge ramp on the tandem cavity response was similar to its effect on the single cavity response. These results are similar to those reported by Carr (Ref 7).

$L/D = 4 \frac{1}{4}$ Cavities. The spectra of the $4 \frac{1}{4}$ inch long

rectangular cavity are presented in Figs. 26 through 30. At $M = 1.5$ the plots consist of two dominant modes and several less predominant modes and other tones. As the flow Mach number is decreased, the mode-1 and mode-2 discrete frequencies become more significant and the higher mode tones degenerate to broadband noise.

The effect of the 45° , 1/2 inch, trailing edge ramp was to raise the level of the mode-1 frequency and reduce the high frequency tones for the supersonic flows. The subsonic spectra were exactly like the spectra for the rectangular cavity. The 45° , 1 inch, rear ramp had a similar, though more powerful, effect. More energy was concentrated in the mode-1 tone and the peaks at higher frequencies are nearly completely eliminated except for low level harmonics of the mode-1 tone. The harmonics on the plots indicate that the mode-1 level had probably reached the microphone limit. The leading edge ramps caused the levels in the cavity to increase beyond the upper limits of the transducers. For this reason, the true spectra and maximum levels are unknown for the cavity with leading edge ramp and higher Mach numbers.

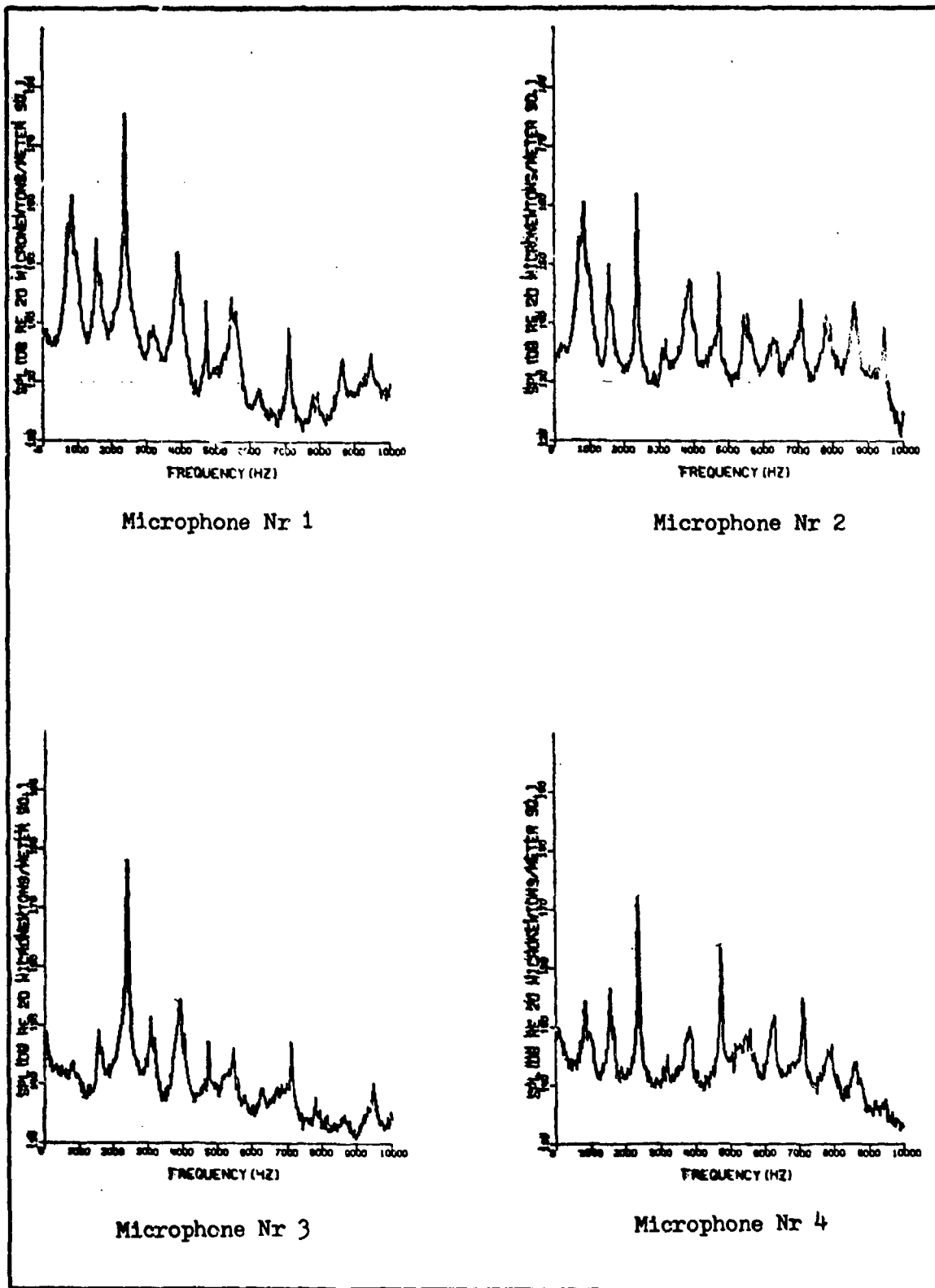


Fig. 26. Sound Pressure Level Variation with Frequency in the $L/D = 4.25$ Rectangular Cavity at $M = 1.5$.

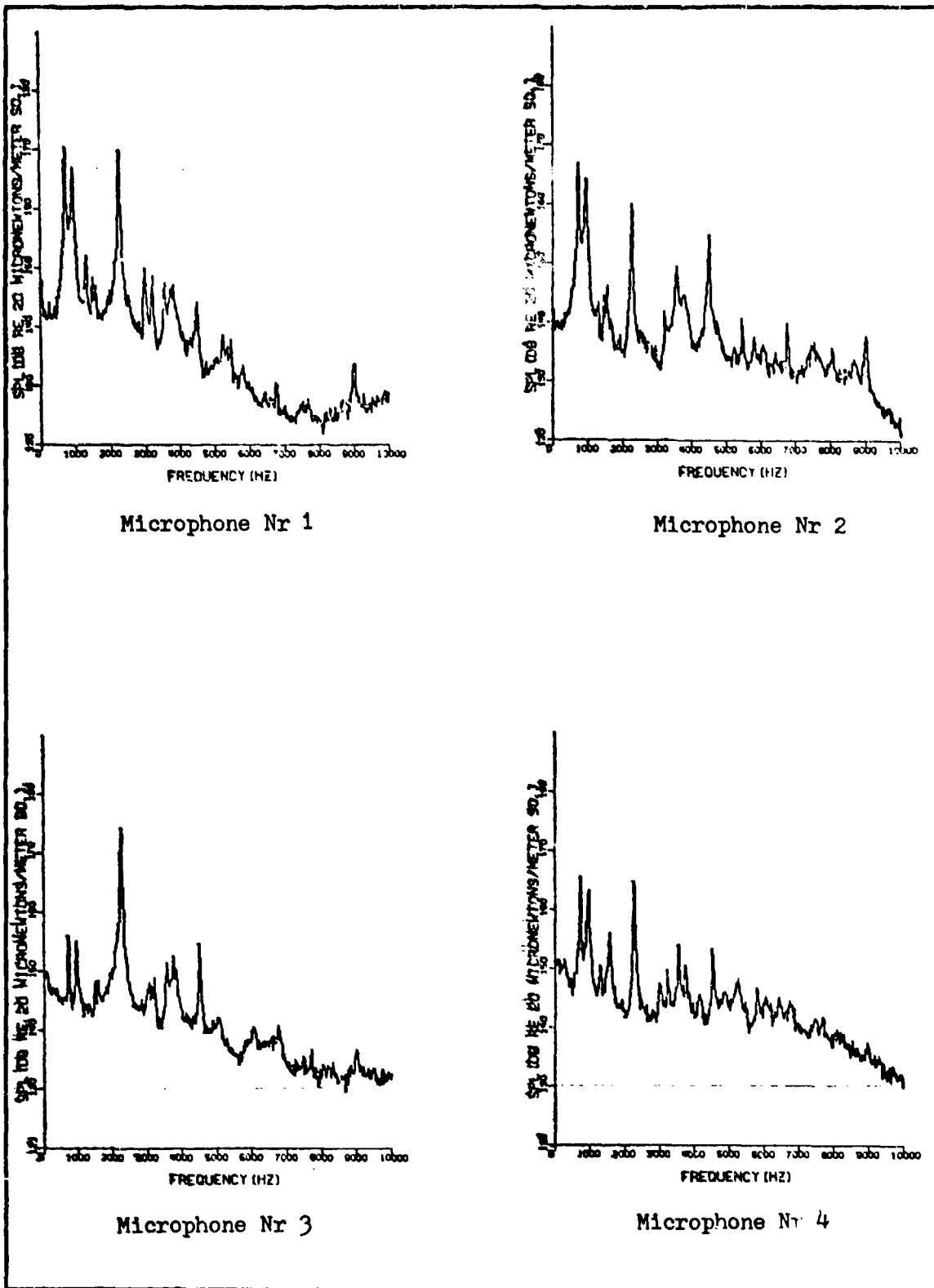


Fig. 27. Sound Pressure Level Variation with Frequency in the $L/D = 4.25$ Rectangular Cavity at $M = 1.3$.

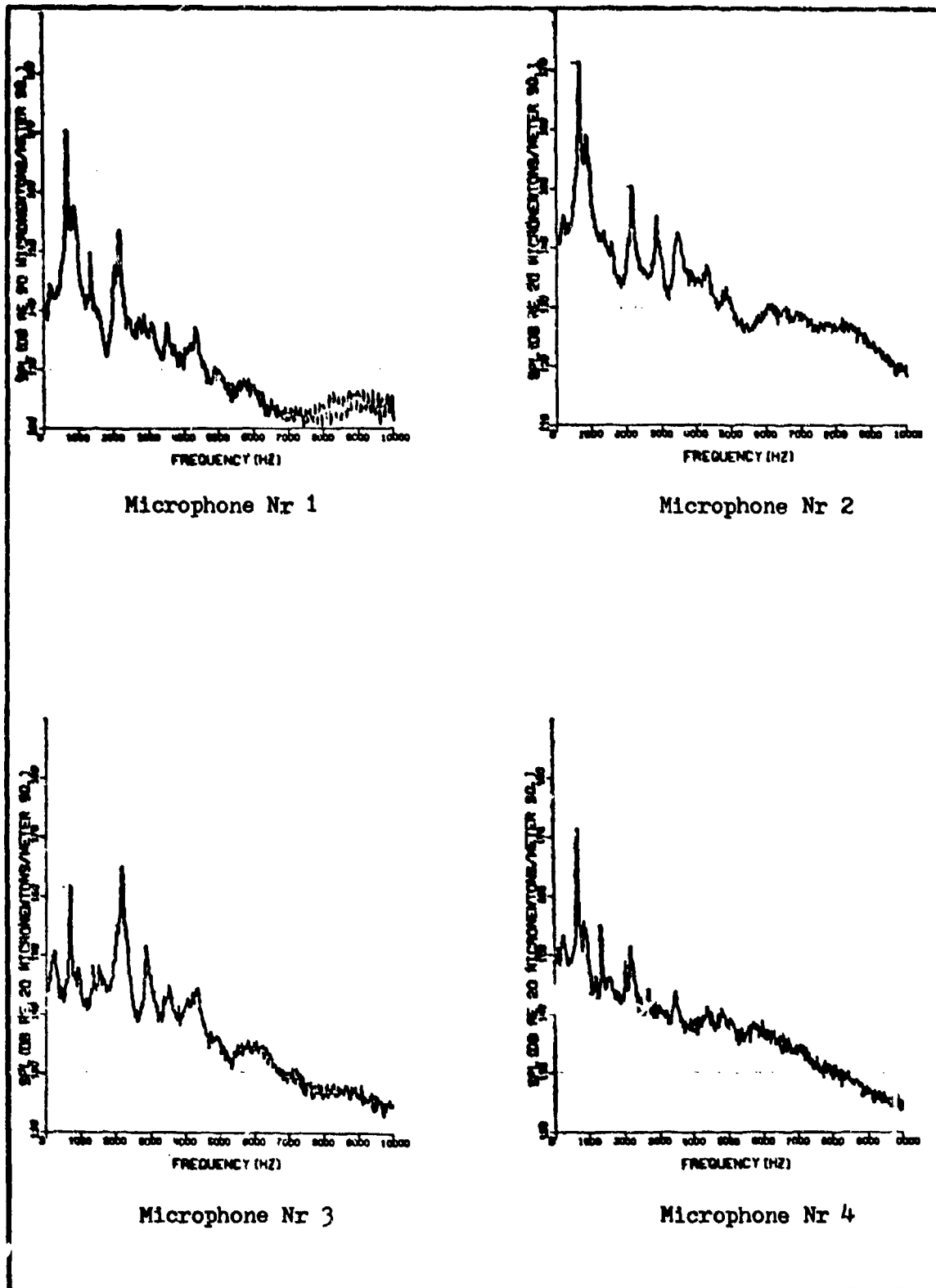


Fig. 28. Sound Pressure Level Variation with Frequency in the $L/D = 4.25$ Rectangular Cavity at $M = 1.0$.

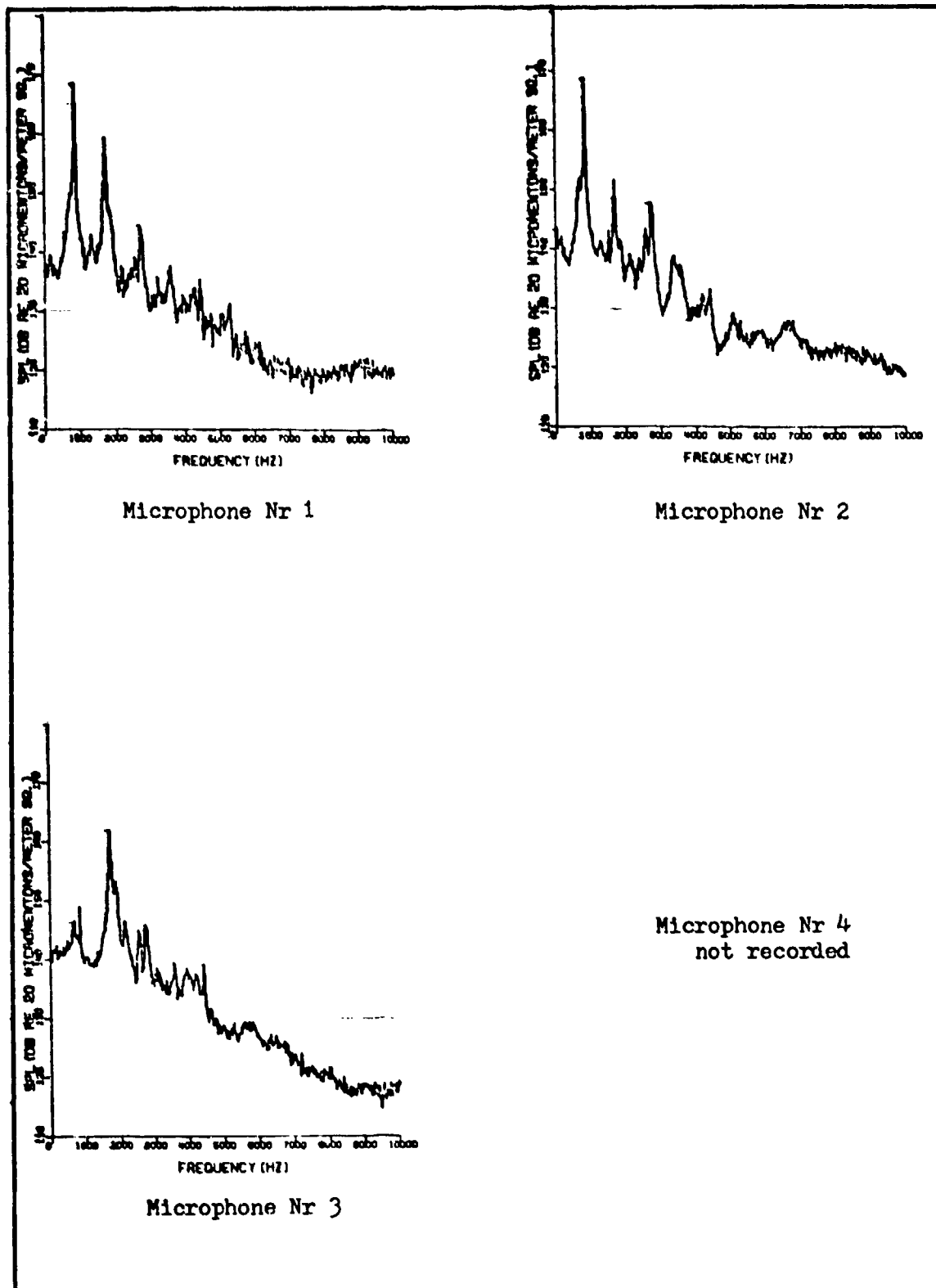


Fig. 29. Sound Pressure Level Variation with Frequency in the $L/D = 4.25$ Rectangular Cavity at $M = 0.6$.

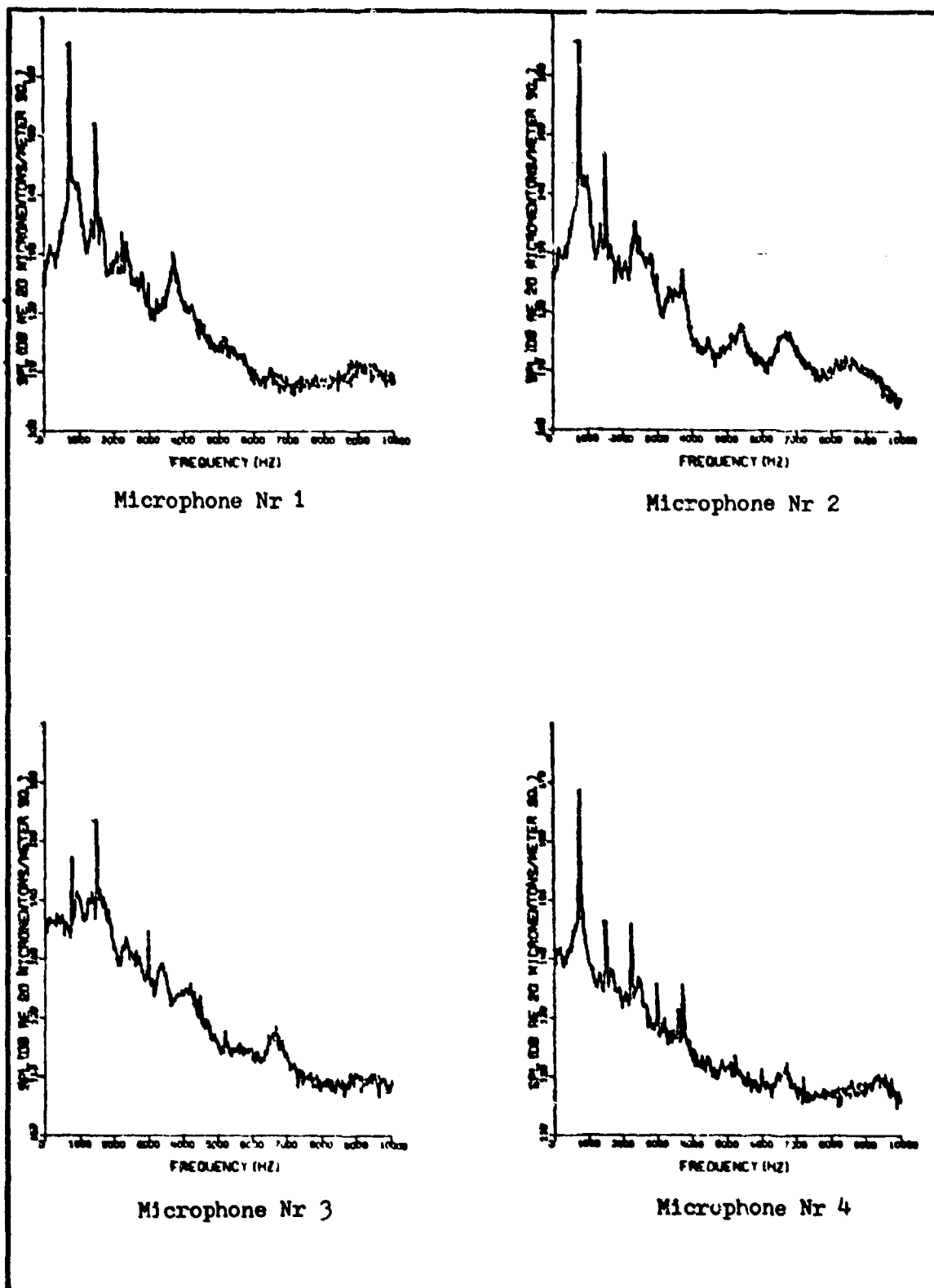


Fig. 30. Sound Pressure Level Variation with Frequency in the $L/D = 4.25$ Rectangular Cavity at $M = 0.5$.

VI. Conclusions

It was found that the relation of Mach number of the flow to the cavity resonant levels fit a previously determined pattern: maximum levels occur at transonic flow velocities. Certain details such as which response mode was dominant were found to be inconsistent with prior tests.

For the short cavity, the relative effectiveness of the trailing edge ramps to suppress resonant oscillations was consistent with previous work. Increasing the ramp angle improved the suppression. The 1/2 inch ramp at 45° did not produce significant suppression compared to the 1 inch ramps. The leading edge ramp was found to be the most effective means to reduce the discrete frequency resonance in the short cavity.

The response of tandem cavities was found to be controlled by the first cavity. Trailing edge ramps used in the second cavity had negligible effects. The leading edge ramp had an effect in both cavities similar to that on the short single cavity response.

The long cavity response was characterized by several primary mode frequencies. The trailing edge ramps tended to reduce the level of higher mode tones while concentrating more energy in the primary modes. The ramps did not reduce the maximum dynamic levels at all Mach numbers. The leading edge ramp was found to augment rather than suppress the response of the long cavity.

Bibliography

1. Karamcheti, K. "Acoustic Radiation from Two-Dimensional Rectangular Cutouts in Aerodynamic Surfaces." National Advisory Committee for Aeronautics Technical Note (NACA TN) 3487, Washington, D.C.: NACA, August 1955.
2. Roshko, A. "Some Measurements of Flow in a Rectangular Cutout." National Advisory Committee for Aerodynamics Technical Note (NACA TN) 3488, August 1955.
3. Mault, D. J. and East, L. F. "Three-Dimensional Flow in Cavities." Journal of Fluid Mechanics, 16:620-632 (August 1963).
4. East, L. F. "Aerodynamically Induced Resonance in Rectangular Cavities." Journal of Sound and Vibration, 3:277-287 (March 1966).
5. Heller, H. and D. Bliss. "Aerodynamically Induced Pressure Oscillations in Cavities: Physical Mechanisms and Suppression Concepts." Technical Report, AFFDL-TR-74-133. Air Force Flight Dynamics Laboratory, Wright-Patterson Air Force Base, Ohio, 1974.
6. Heller, H., S. Widnall, J. Jones, and D. Bliss. "Water-Table Visualization of Flow-Induced Pressure Oscillations in Shallow Cavities for Simulated Supersonic Flow Conditions." Paper Z13, presented at 86th Meeting, Acoustical Society of America, 1973.
7. Carr, D. L. An Experimental Investigation of Open Cavity Pressure Oscillations. Unpublished Thesis. Wright-Patterson Air Force Base, Ohio: Air Force Institute of Technology, December 1974.
8. Charwat, A. F., et al. "An Investigation of Separated Flows - Part I: The Pressure Field." Journal of Aerospace Sciences, 28:457-470 (June 1961).
9. Heller, H., G. Holmes, and E. Covert. "Flow Induced Pressure Oscillations in Shallow Cavities." Technical Report, AFFDL-TR-70-104. Air Force Flight Dynamics Laboratory, Wright-Patterson Air Force Base, Ohio, 1970.
10. Franke, M. E. and D. L. Carr. "Effect of Geometry on Open Cavity Flow-Induced Pressure Oscillations." Paper 75-492, presented at the American Institute of Aeronautics and Astronautics 2nd Aero-Acoustics Conference, Hampton, Virginia, March 24-26, 1975.

Vita

Michael Floyd Marquardt was born 20 September 1946 in Wabasha, Minnesota. He was graduated from the University of Minnesota with a Bachelor of Aeronautical Engineering degree in 1969. He received his commission through the Reserve Officer Training Corps program. His first assignment was as a foreign aircraft analyst in the Foreign Technology Division. He entered the Air Force Institute of Technology in May 1974.

Permanent address: 835 Franklin Avenue
Wabasha, Minnesota 55981

This thesis was typed by Arlene Marquardt.